METEORITE CONCENTRATION BY ICE FLOW

by

Marijke van Heeswijk

Honors Thesis
presented in partial fulfillment of
the requirements for the degree of
Bachelor of Science
with distinction in
Geology and Mineralogy

The Ohio State University
Spring, 1983

Approved by:

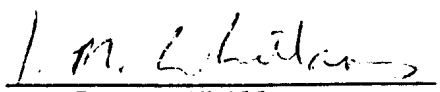

Dr. Ian M. Whillans
Advisor

TABLE OF CONTENTS

ABSTRACT

Ice flow concentrates meteorites and supplies old ice at the ablation surface near the Allan Hills, Antarctica. A model for these phenomena is proposed by Whillans and Cassidy, and is developed in this paper. The model recognizes three mechanisms that act to concentrate the meteorites: some meteorites fall directly onto the collecting site, others are transported by the glacier from the accumulation to the ablation zone, and those present at the ablation surface are crowded due to horizontally-compressive surface strain rates.

Large meteorite concentrations and old ice are favored by the following conditions: thick ice, slow velocities, convergent flow, low accumulation and ablation rates, large ablation area, and steep velocity profiles.

Calculations show that ice as old as 160,000 years could be present at the ablation surface near the Allan Hills. Ice this old has never been found before.

ACKNOWLEDGEMENTS

I thank my advisor, Ian Whillans, for giving me the opportunity to do this project and the guidance to see it to completion. To my amazement, he always made time for an additional counseling session, many times at 5 o'clock on friday afternoon. His help and patience were boundless.

In addition I thank G. Faure and G. Newsom for serving on my committee and offering helpful suggestions. My officemates Richard Alley and John Bolzan were always willing to discuss questions and thoughts that arose at the spur of the moment.

I thank Joni Wood for typing this report, and Tom DeVries for the encouragement to never give up. I am grateful to my parents for making it possible for me to study in the United States and for being supportive throughout my stay here.

All these people gave more support than they could ever know.

This project was funded by an Undergraduate Research Scholarship awarded by The Ohio State University College of the Arts and Sciences Honors Office.

LIST OF FIGURES

LIST OF TABLES

CHAPTER ONE

INTRODUCTION

Since the early 1970's scientists have been finding unusually large numbers of meteorites at two locations on the East Antarctic ice sheet. The first site was discovered near the Yamato Mountains by Japanese scientists during the 1969-1970 field season (Yoshida et al., 1971). A second site was discovered near the Allan Hills by a joint U.S.-Japanese expedition in the mid 1970's (Cassidy et al., 1977; Yanai, 1978). So far, more than 5000 meteorites have been found in Antarctica (Nishiizumi et al., 1981). Before these discoveries, only 2000 had been collected in the entire world (Cassidy et al., 1982).

The Yamato Mountains and Allan Hills (see Figure 1) are adjacent to regions of bare ice (also referred to as blue ice) on which meteorites are exposed. These meteorites are of all major types (stony, stony-iron, and iron) and most have terrestrial ages ranging from 400,000 years until recent. One of the meteorites, however, has a terrestrial age of 700,000 years (Nishiizumi et al., 1979). Both the diversity in age and type of the meteorites suggest they are derived from independent meteorite showers.

Some process must have been in effect for a long time to concentrate these meteorites at the two locations. The behavior of the ice sheet at either site is probably responsible for the high meteorite occurrences.

The East Antarctic ice sheet flows radially from a central area on the continent toward the surrounding ocean. As the sheet flows toward the sea meteorites fall on it and are buried under the accumulation of

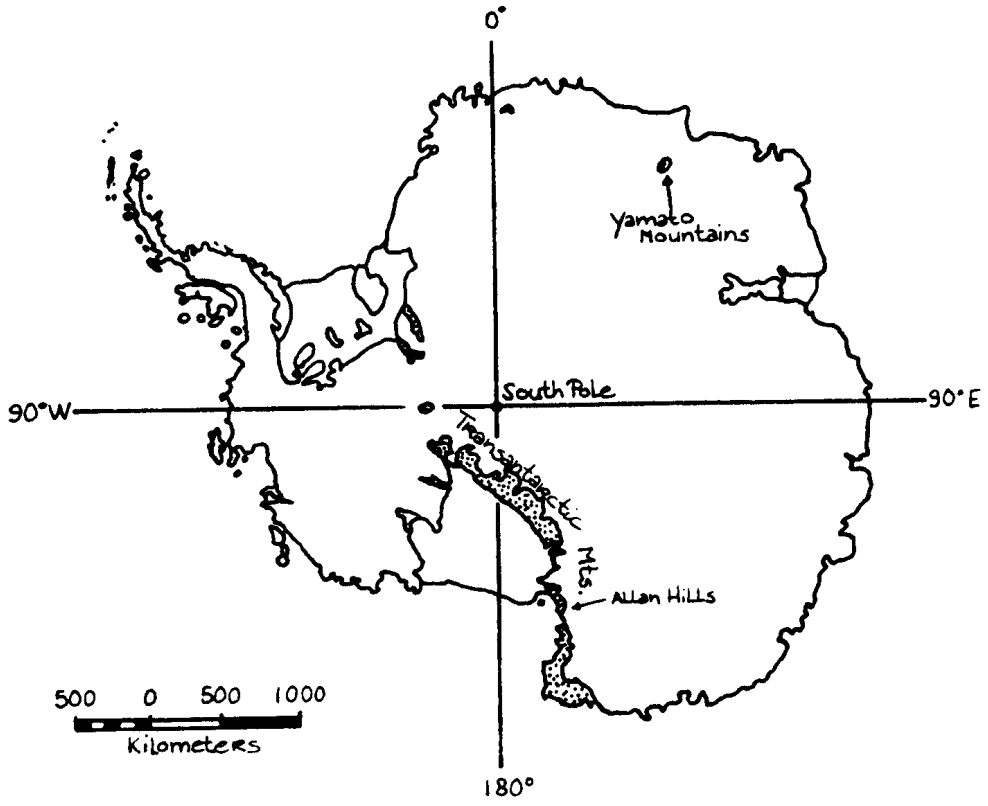

Figure 1. Map of Antarctica showing the locations of the Allan Hills and Yamato Mountains (modified from Cassidy et al., 1977).

snow. At the edge of the ocean parts of it break off to form icebergs that drift into warmer waters. There they melt, and meteorites drop to the ocean floor, no longer easily accessible to scientists and not particularly concentrated. On the other hand, at the Allan Hills and Yamato Mountains the glacial flow is obstructed by mountains, causing the meteorites to be trapped and concentrated.

Nagata (1978) was the first to propose an ice flow model to explain the meteorite concentration in the Yamato Mountains. In 1982 Nishio and others did the same for the Allan Hills. Whillans and Cassidy (in press) propose a different model for the Allan Hills. Their model is similar to Nagata's and Nishio's in that it recognizes the transport of meteorites by the glacier from the accumulation to the ablation zone as an important mechanism to concentrate the meteorites. Whillans and Cassidy, however, find two additional mechanisms to be important and think the concentrating mechanisms have been acting for a much longer time than Nishio and others suggest. All three mechanisms considered by Whillans and Cassidy are described in Chapter 2.

This thesis develops Whillans' and Cassidy's model in detail, describes what the high meteorite concentration means for the age of the ice in the Allan Hills and determines what physical parameters are most important in order to obtain large concentrations of meteorites and old ice.

CHAPTER TWO

MODEL OF METEORITE CONCENTRATION IN THE ALLAN HILLS

Whillans' and Cassidy's model allows one to calculate the expected meteorite concentrations in various parts of the Allan Hills area. Very few data are available from the Allan Hills; ablation rates, strain rates and surface velocities of the glacier have been measured only in a small area close to the Allan Hills glacier snout (Nishio and Annexstad, 1980). In spite of this lack of data, calculations using the model will be made in this thesis using estimated values for the unknowns.

The model argues that there are three mechanisms that act to concentrate the meteorites (see Figure 2). Firstly, some of the meteorites found near the Allan Hills have fallen onto the area directly. The meteorite infall rate is denoted by f.

Secondly, meteorites that fall in the accumulation zone are buried by accumulating snow. From there the meteorites are transported by the glacier to the ablation zone where they reappear at the glacier's surface. In the accumulation zone the concentration of meteorites in the glacier is $\frac{f}{\dot{b}_{ac}}$, where $\dot{b}_{ac}$ is the snow accumulation rate. The rate at which meteorites reappear at the surface in the ablation zone is $\frac{f}{\dot{b}_{ac}} \dot{b}_{ab}$, where $\dot{b}_{ab}$ is the ablation rate.

Thirdly, meteorites that are present at the glacier's surface (because of the workings of the first and second mechanism) are crowded due to horizontal compressive strain rates. The sum of the horizontal strain rates at the surface of the glacier is denoted by $\dot{\varepsilon}_{sx,sy}$ and the concentration of meteorites already present by M. Because $\dot{\varepsilon}_{sx,sy}$ is

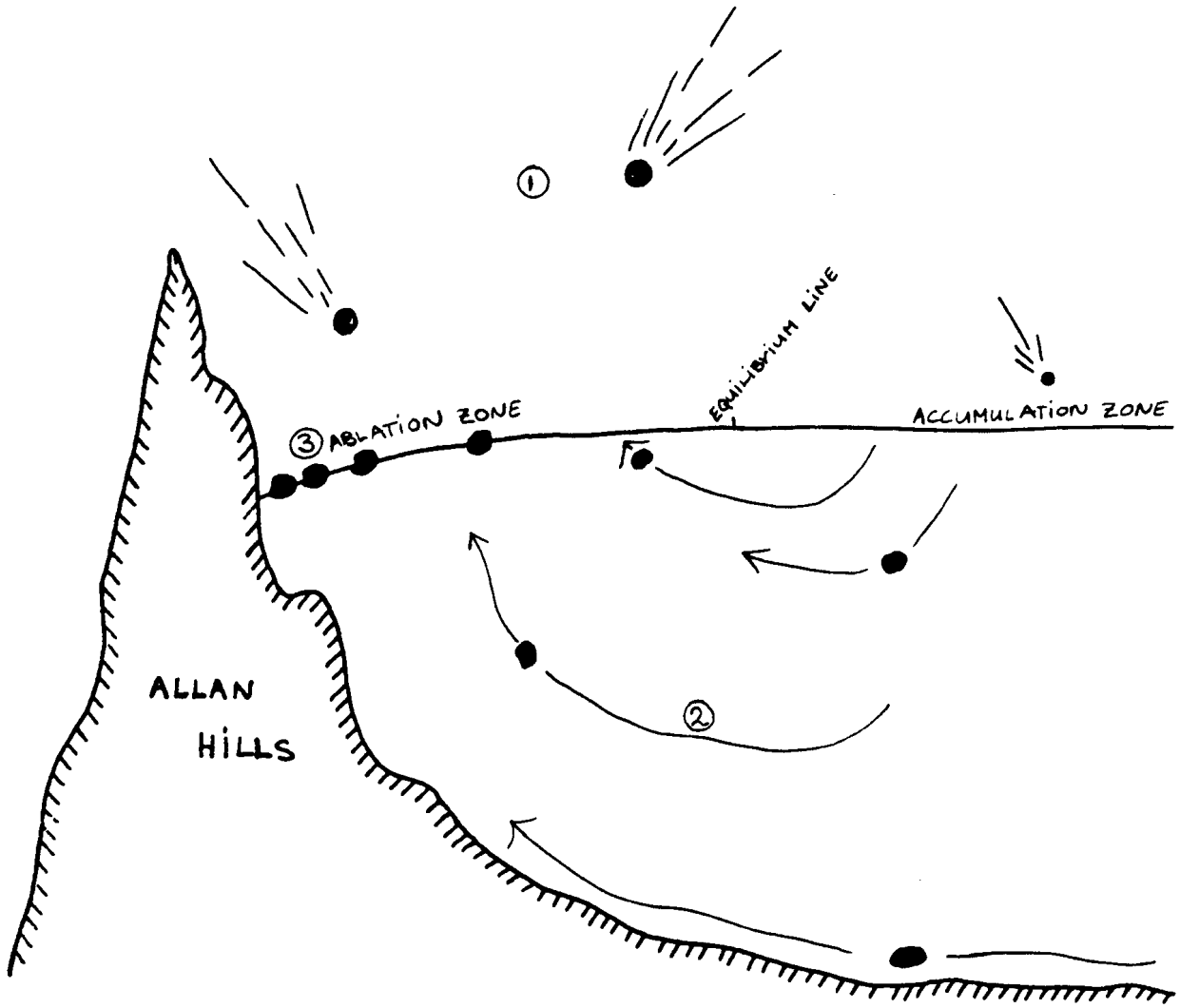

Figure 2. Profile of the glacier near the Allan Hills showing the meteorite concentrating mechanisms.

1. meteorites fall directly onto the ablation zone
2. meteorites that fell in the accumulation zone are transported to the ice surface in the ablation zone.
3. meteorites present at the surface in the ablation zone are crowded due to compressive horizontal strain rates.

(after Whillans and Cassidy, in press)

negative for compressive strain rates for which the third mechanism acts to increase the meteorite concentration, crowding is expressed as $-\dot{\varepsilon}_{sx,sy}M$.

All three mechanisms described above act to concentrate meteorites in the ablation zone. The summed effects of all three mechanisms determine how the meteorite concentration at the ablation surface changes with time. The meteorite infall rate f, the ablation rate $\dot{b}_{ab}$, and the accumulation rate $\dot{b}_{ac}$ are assumed constant through time, but the concentration of meteorites already present in the ablation area (M) and the sum of the horizontal strain rates ($\dot{\varepsilon}_{sx,sy}$) are allowed to vary through time. Therefore, the change in meteorite concentration through time in the Allan Hills ablation area can be expressed as:

$$\frac{dM(t)}{dt} = \frac{f}{\dot{b}_{ac}} \dot{b}_{ab} + f - \dot{\varepsilon}_{sx,sy}(t)M(t) \qquad (1)$$

It is easier to work with the meteorite concentration M(t) as varying with distance instead of time. Because Whillans' and Cassidy's model is for a steady-state glacier, quantities can be expressed as a function of distance, x, instead of time, t. This changes $\dot{\varepsilon}_{sx,sy}(t)$ to $\dot{\varepsilon}_{sx,sy}(x)$ and M(t) to M(x). Both sides of equation (1) are multiplied by the reciprocal of the surface velocity of the glacier in the x-direction $u_{sx}(x)$, which is a function of distance from the snout (x) and is equivalent to $\frac{dt}{dx}$. When the substitutions and multiplication are carried out, expression (1) changes to:

$$\frac{dM(x)}{dx} = \left\{\frac{f}{\dot{b}_{ac}} \dot{b}_{ab} + f - \dot{\varepsilon}_{sx,sy}(x)M(x)\right\} / u_{sx}(x) \qquad (2),$$

so that now the meteorite concentration is expressed as varying with distance from the glacier snout instead of time.

Equation (2) is a differential equation that is to be solved for the meteorite concentration M(x). A finite differenced approximation for this equation is derived in Appendix B. Since quantities f, $\dot{b}_{ac}$ and $\dot{b}_{ab}$ are assumed constant, and x is arbitrarily chosen, only surface velocity $u_{sx}(x)$ and sum of horizontal surface strain rates $\dot{\varepsilon}_{sx,sy}(x)$ need to be found.

An expression for the surface velocity $u_{sx}(x)$ is found using a version of the equation of continuity of ice flow described by Whillans in 1977. If all terms in this equation are divided by the mean density of ice, the change in thickness with time ($\dot{z}$) of a glacier equals the mass balance of the glacier ($\dot{b}$) minus the horizontal divergence of the flux. The flux is the thickness of the glacier z times the mean horizontal ice velocity $\bar{u}$ through vertical planes perpendicular and parallel to the direction of ice flow. Mathematically this version of the equation of continuity of ice flow is expressed as:

$$\dot{z} = \dot{b} - \nabla \cdot z\bar{u} \tag{3}$$

Thickness z, mean horizontal velocity $\bar{u}$ and mass balance $\dot{b}$ are functions of distance x from the snout. For clarity in the derivation of $u_{sx}(x)$, however, the function variable x is omitted from notations in the derivation below.

Del (∇) is treated as vector $\frac{\partial}{\partial x}\vec{i} + \frac{\partial}{\partial y}\vec{j}$ and expression (3) is expanded to:

$$\dot{z} - \dot{b} = -(\frac{\partial}{\partial x}\vec{i} + \frac{\partial}{\partial y}\vec{j}) \cdot (z\bar{u}_x\vec{i} + z\bar{u}_y\vec{j}),$$

where subscripts x and y refer to the horizontal axes parallel and perpendicular to the direction of ice flow respectively. Further expansion gives:

$$\dot{z} - \dot{b} = - \frac{\partial}{\partial x}(z\bar{u}_x) - \frac{\partial}{\partial y}(z\bar{u}_y),$$

which simplifies to :

$$\partial (z\bar{u}_x) = (\dot{b} - \dot{z} - \frac{\partial}{\partial y}(z\bar{u}_y))\partial x. \qquad (4)$$

To find an expression for the surface velocity $u_{sx}(x)$, additional alterations are made to equation (4). Both sides of this equation are differentials that are integrated. The lower limits of integration are chosen as zero and the upper limits as the general quantities with respect to which each side of the equation is integrated. In addition, the term $\frac{\partial}{\partial y}(z\bar{u}_y)$ at the right hand side of expression (4) is expanded to $z\frac{\partial \bar{u}_y}{\partial y} + \bar{u}_y\frac{\partial z}{\partial y}$. As noted above, the x-axis is defined parallel to the direction of ice flow, which means that the mean velocity in the y-direction $(\bar{u}_y)$ at y=0 equals zero. The partial derivative of this velocity, $\frac{\partial \bar{u}_y}{\partial y}$, is not necessarily equal to zero, because nearby flowlines need not be parallel to the x-axis. Therefore, term $\frac{\partial}{\partial y}(z\bar{u}_y)$ is substituted by $z\frac{\partial \bar{u}_y}{\partial y}$. Now the integral equivalent of expression (4) becomes:

$$\int_0^{z\bar{u}_x} \partial(z\bar{u}_x) = \int_0^x (\dot{b} - \dot{z} - z\frac{\partial \bar{u}_y}{\partial y})\partial x. \qquad (5)$$

Mean lateral strain rate $\bar{\dot{\varepsilon}}_y$ is equal to the change in mean velocity in the y-direction per distance step $(\frac{\partial \bar{u}_y}{\partial y})$ (Paterson, 1981, p. 65). This equality is substituted into expression (5), which changes to

$$\bar{u}_x = \frac{1}{z}\int_0^x (\dot{b} - \dot{z} - z\bar{\dot{\varepsilon}}_y)\partial x \qquad (6)$$

after the integration of the left hand side is carried out and both sides of the resulting expression are divided by thickness z of the glacier. Equation (6) gives an expression for the mean velocity through the glacier in the x-direction. The objective of the derivation above, however, is to find an expression for u_{sx}, the horizontal surface velocity in the x-direction.

Whillans (1977) states that mean velocity and mean strain rate are related to their mean values at particular depths into the glacier by a factor ψ. This factor is a function of depth into the glacier and is denoted by $\psi(o)$ at the surface. Therefore, the surface velocity in the x-direction is expressed as:

$$u_{sx} = \psi(o)\ \bar{u}_x, \tag{7}$$

and the surface strain rate in either the x or y-direction as:

$$\dot{\varepsilon}_s = \psi(o)\bar{\dot{\varepsilon}}. \tag{8}$$

In the extreme case where all glacier flow takes place by internal deformation with no contribution of basal sliding, ψ will be zero at the glacier/bed interface. An expression for ψ is given in chapter 3, and this expression has been determined empirically.

Now that relationships between surface and mean values for velocity and strain rate are known, substitution of expressions (7) and (8) into (6) gives:

$$u_{sx} = \frac{1}{z} \int_o^x \left\{(\dot{b} - \dot{z})\psi(o) - z\dot{\varepsilon}_{sy}\right\} \partial x,$$

which can be written as

$$u_{sx}(x) = \frac{1}{z(x)} \int_o^x \left\{(\dot{b}(x) - \dot{z})\psi(o) - z(x)\dot{\varepsilon}_{sy}(x)\right\} \partial x \tag{9}$$

if the function-variable x (distance from the snout) is no longer omitted. Mass balance $\dot{b}(x)$, change in thickness $\dot{z}$ and factor $\psi(o)$ are taken as known at various distances from the snout. Thickness z(x) is approximated by

$$z(x) = ax^{1/Q} - \dot{z}(t_o - t) \quad \text{for } x \leq x_{eq} \tag{10a}$$

and by

$$z(x) = ax_{eq}^{1/Q} - \dot{z}(t_o - t) \quad \text{for } x \geq x_{eq} \tag{10b}$$

at various distances from the snout (Whillans, 1982; pers. comm.).

In expression (10a) and (10b), Q and a are constants that determine the shape of the glacier profile, x_{eq} is the distance from the snout to the equilibrium line, $\dot{z}$ (as for expression (9)) is the rate of change in thickness, t_o is a constant and t represents time. Term $\dot{z}(t_o - t)$ has no significance for a steady state profile, because then $\dot{z}$ equals zero.

Lateral surface strain rate $\dot{\varepsilon}_{sy}(x)$ is not known in expression (9), but is approximated by $\frac{|u_{sx}(x)|}{R}$. Term $|u_{sx}(x)|$ is the absolute value of the ice velocity in the x-direction along the glacier, and R is the radius of curvature of ice elevation contours. An explanation for this substitution is given in Appendix A.

Equation (10) causes the ice thickness profile to be smoother than it is in reality as can be seen in Figure 3. This figure shows a profile produced by equation (10) and parts of one derived from data obtained by Drewry (1975, 1977). Most of the discrepancy between the profiles is because equation (10) is based on a profile along a different flowline. Figure 4 shows a map view of the Allan Hills area and the location of the two flowlines chosen that resulted in the different ice thickness profiles of Figure 3.

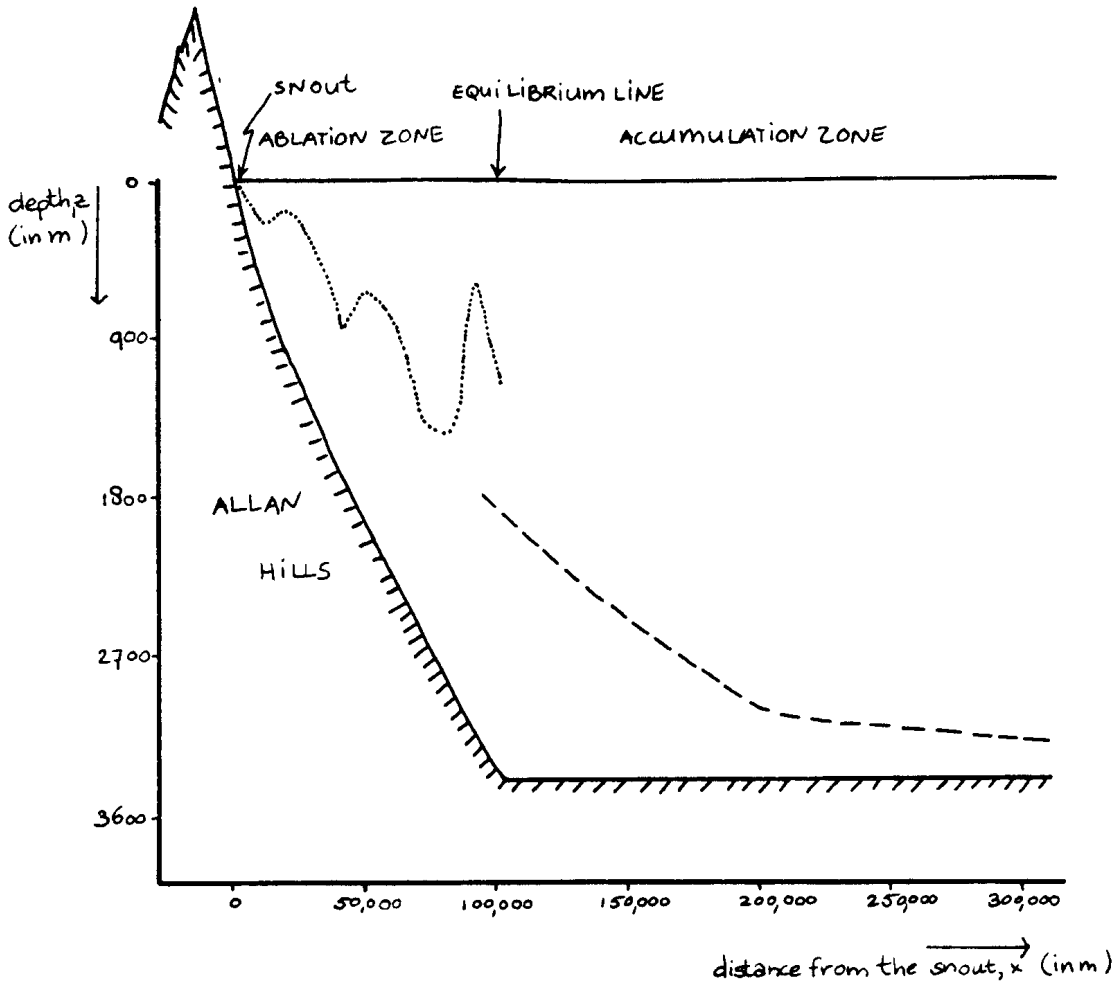

Figure 3. Ice thickness profiles. Vertical exaggeration is about 67 times.
———: bed boundary as produced by equation (10a) and (10b)
·····: bed boundary derived from Drewry (1977)
— — —: bed boundary derived from Drewry (1975)

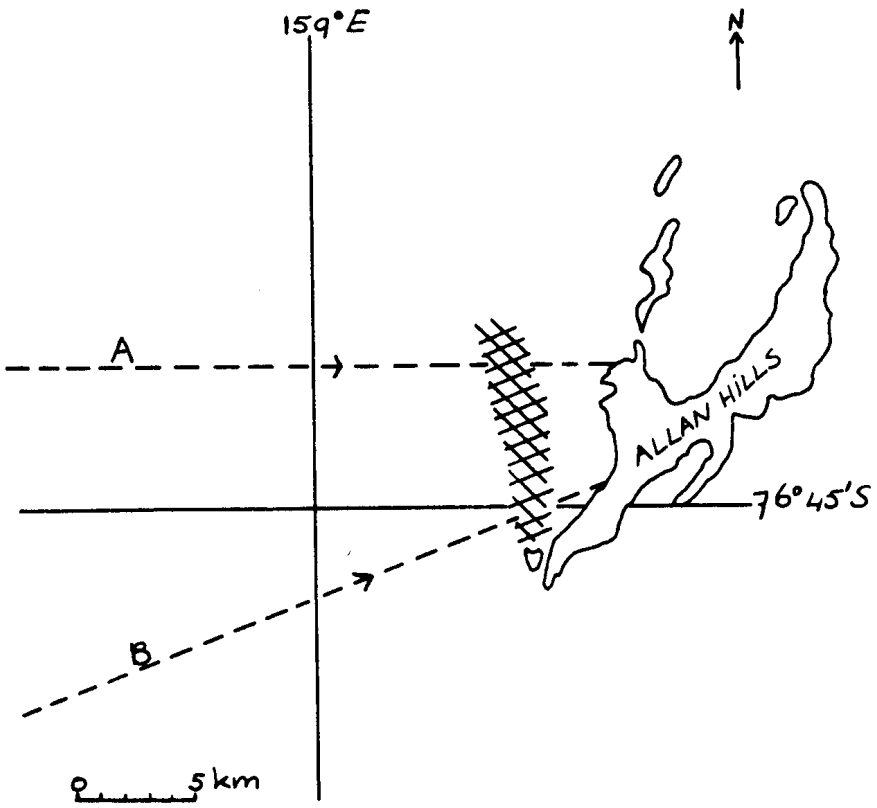

Figure 4. Map view of the Allan Hills area. The ice thickness profile generated by equations (10a) and (10b) is under flowline A, and the second profile is approximately located under flowline B. Meteorites have been found in the shaded area. (Map modified from Fireman and Norris, 1982)

An expression for $\dot{\varepsilon}_{sx,sy}$ is found using the same version of Whillans' equation for continuity of ice flow (1977) as used above to find an expression for surface velocity $u_{sx}(x)$. Whillans' equation is expanded above to

$$\dot{z} - \dot{b} = -\frac{\partial}{\partial x}(z\bar{u}_x) - \frac{\partial}{\partial y}(z\bar{u}_y),$$

which is equivalent to

$$\dot{z} - \dot{b} = -z\frac{\partial \bar{u}_x}{\partial x} - \bar{u}_x \frac{\partial z}{\partial x} - z\frac{\partial \bar{u}_y}{\partial y} - \bar{u}_y \frac{\partial z}{\partial y}. \qquad (11)$$

Switching terms between the left hand side and right hand side of expression (11) and dividing both sides by thickness z gives

$$\frac{\partial \bar{u}_x}{\partial x} + \frac{\partial \bar{u}_y}{\partial y} = \frac{1}{z}\left(-\bar{u}_x\frac{\partial z}{\partial x} - \bar{u}_y\frac{\partial z}{\partial y} + \dot{b} - \dot{z}\right). \qquad (12)$$

According to Paterson (1981, p. 65) $\frac{\partial \bar{u}_x}{\partial x} + \frac{\partial \bar{u}_y}{\partial y}$ equals the sum of the mean strain rates in the x and y-direction, $\bar{\dot{\varepsilon}}_{x,y}$. The x-axis is defined such that the mean velocity in the y-direction ($\bar{u}_y$) equals zero. As mentioned above, however, this does not mean that the partial derivative of this velocity, $\frac{\partial \bar{u}_y}{\partial y}$, equals zero, because nearby flowlines need not be parallel to the x-axis.

Equation (12) then becomes

$$\bar{\dot{\varepsilon}}_{x,y} = \frac{1}{z}\left(-\bar{u}_x\frac{\partial z}{\partial x} + \dot{b} - \dot{z}\right) \qquad (13),$$

which is the sum of the horizontal strain rates meaned through the thickness.

Equation (2), however, requires surface values. Surface values are related to mean values by equation (7) and (8). Substituting these relationships, expression (13) results in

$$\dot{\varepsilon}_{sx,sy} = \frac{1}{z}\left\{-u_{sx}\frac{\partial z}{\partial x} + (\dot{b} - \dot{z})\ \psi(o)\right\},$$

which changes to

$$\dot{\varepsilon}_{sx,sy}(x) = \frac{1}{z(x)}\left\{-u_{sx}(x)\frac{\partial z(x)}{\partial x} + (\dot{b}(x) - \dot{z})\psi(o)\right\} \qquad (14)$$

if function variable x is attached to appropriate variables.

In equation (14) z(x) represents the thickness of the glacier and can be approximated at various distances from the snout by expressions (10a) and (10b) above. Mass balance $\dot{b}(x)$, change in thickness $\dot{z}$ and factor $\psi(o)$ are taken as known at various distances from the snout. Partial derivative $\frac{\partial z(x)}{\partial x}$ is found from equations (10a) and (10b). A substitution for the partial derivative is not made at this point, but is made in Appendix A, where additional alterations are made in equation (14) to make it more suitable for use in a computer program. An expression for the surface velocity in the x-direction $u_{sx}(x)$ is given by equation (9).

In summary, Whillans' and Cassidy's model to explain the meteorite concentration in the Allan Hills can be represented by one differential equation ((2) above), which can be solved if expressions for horizontal surface velocity in the x-direction $u_{sx}(x)$ and sum of horizontal surface strain rates $\dot{\varepsilon}_{sx,sy}$ are known. Equations for both unknowns have been derived above and are equation (9) for $u_{sx}(x)$ and equation (14) for $\dot{\varepsilon}_{sx,sy}$. Equation (9) needs to be solved before a solution to equation (14) can be found. Both equations undergo slight additional alterations in Appendices B and A respectively; equation (9) is approximated by a finite differenced form, and substitutions are made in equation (14).

In Appendix C a computer program is listed that uses the model explained above to calculate expected meteorite concentrations at various distances from the snout in the Allan Hills, using parameters

suggested by Whillans and Cassidy (in press). A sample output of the program in Appendix C and accompanying graphs are listed in Appendix D.

CHAPTER THREE

DEPTHS AND AGES OF ICE NEAR THE ALLAN HILLS

The model developed in Chapter 2 enables one to calculate expected meteorite concentrations in the Allan Hills. It is based on the understanding that ice with meteorites embedded in it flows from the surface of the accumulation zone down into the glacier and back up again to reappear at the surface in the ablation zone near the Allan Hills. Flowlines for such paths are shown in Figure 5, which is a graph of one of the sample outputs of the program listed in Appendix C. An interesting result from this flow pattern is that not only do meteorites of different terrestrial ages surface in the ablation zone, but also ice of different ages. Possible ages for ice on the glacier surface at various distances from the Allan Hills are calculated using the theory developed in this chapter describing how the depth of a particle changes as it travels along a flowline.

Consider a thin layer of ice of thickness λ at some depth z in the glacier. This layer is within the accumulation zone at a certain distance from the glacier snout and travels along a flowline towards the snout. It travels distance dx during a short period of time dt, and becomes compressed vertically. This is because vertical strain rates are usually compressive in an accumulation zone (Paterson, 1981, p. 65). Representing the vertical strain rate at the depth of the layer by $\dot{\varepsilon}_z(z)$, the thinning of the original layer of thickness λ by $d\lambda$ after time dt is expressed as:

$$d\lambda = \dot{\varepsilon}_z(z)\ \lambda\ dt. \qquad (1)$$

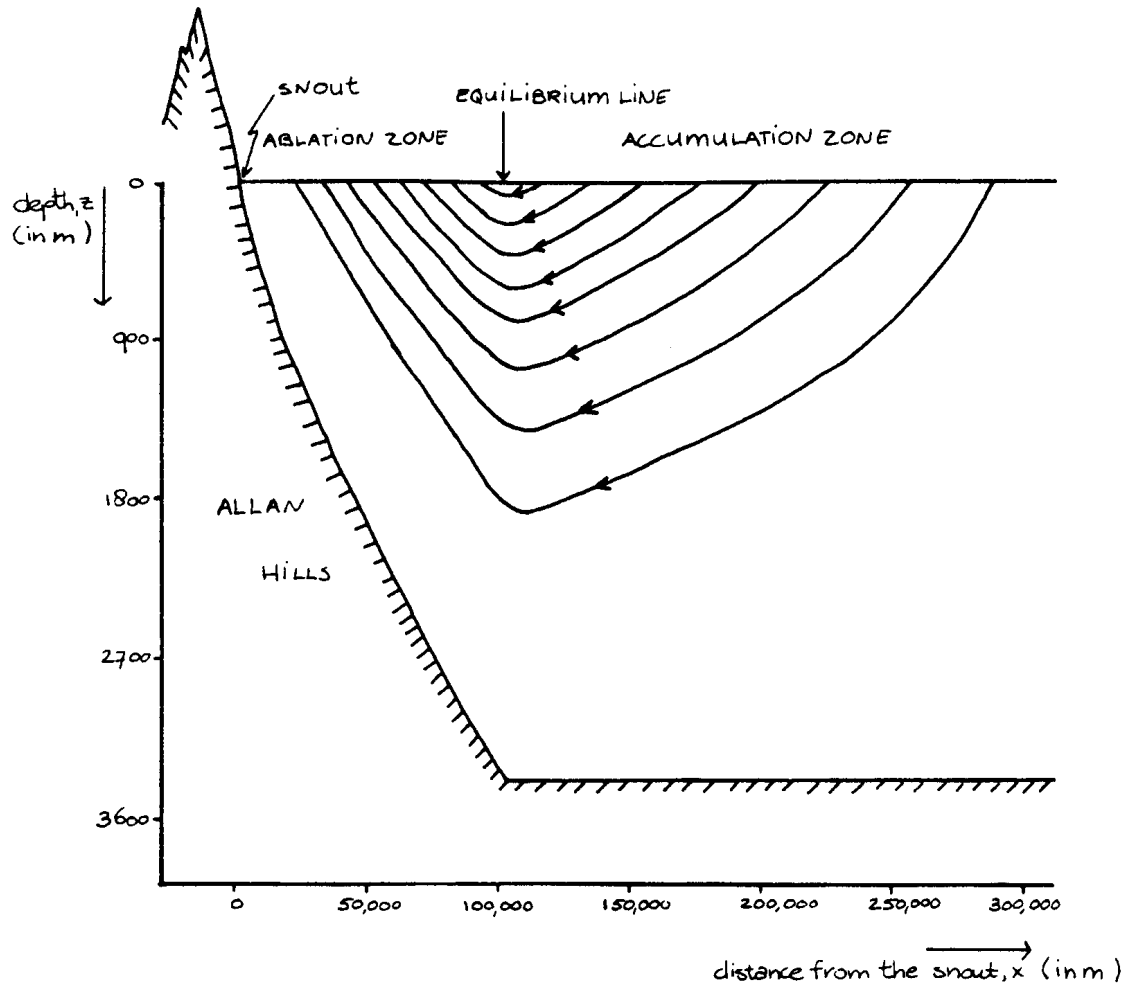

Figure 5. Particle trajectories. Vertical exaggeration is about 67 times.

The time dt it takes the layer to travel distance dx is $dx/u_x(z)$, where $u_x(z)$ is the velocity in the x-direction of the layer at depth z. Substitution of this into expression (1) yields

$$d\lambda = \dot{\varepsilon}_z(z)\lambda \frac{dx}{u_x(z)} \qquad (2),$$

which expresses thinning as a function of depth and distance, instead of depth and time.

Both the vertical strain rate $\dot{\varepsilon}_z$ and velocity in the x-direction u_x at depth z in the glacier are related to their mean values through the glacier by a factor ψ. This relationship was discussed earlier in Chapter 2, and is expressed as

$$\dot{\varepsilon}_z(z) = \psi(z)\bar{\dot{\varepsilon}}_z \qquad (3),$$

where $\bar{\dot{\varepsilon}}_z$ is the mean vertical strain rate, and as

$$u_x(z) = \psi(z)\,\bar{u}_x \qquad (4),$$

where $\bar{u}_x$ is the mean velocity in the x-direction. When equations (3) and (4) are substituted into expression (2), it changes to

$$d\lambda = \frac{\bar{\dot{\varepsilon}}_z}{\bar{u}_x}\lambda\, dx \qquad (5),$$

because factor $\psi(z)$ cancels after the substitution is made. Equation (5) describes the thinning of the layer as it travels a distance dx and it is no longer dependent on depth, but retains a distance dependence.

The latter observation has an important implication. It means that equation (5) does not just describe what happens to a layer of ice of small thickness λ at some depth z, but the equation also describes how much a thick layer λ above a particle at some depth z thins, after the particle and the layer above it have travelled a distance dx. Replacing λ by z in expression (5), $\frac{\dot{\varepsilon}_z}{\bar{u}_x}\, z\, dx$ describes how the depth of a particle

changes under the influence of vertical strain rates as it travels along a flowline.

The change in depth of a particle is not only due to the effect of vertical strain rates, but also due to that of mass balance $\dot{b}$. In the accumulation zone, snow (which changes to ice shortly after depostion) continues to accumulate at a rate $\dot{b}_{ac}$ while a particle and the ice above it travel distance dx. After a short period of time dt, the ice thickness z is increased by an ice layer of thickness $\dot{b}_{ac}dt$. As before, dt is replaced by $dx/u_x(z)$, where dx is the distance travelled along the flowline and $u_x(z)$ the speed at which the particle travels. Because the calculations follow a trajectory at depth, it is the time of travel, dt $= dx/u_x(z)$, at that depth that is used here. Substituting expression (4) for $u_x(z)$, the thickness z′ of the ice layer added is:

$$z' = \frac{\dot{b}_{ac}dx}{\bar{u}_x\psi(z)} \quad . \tag{6}$$

In expression (6) $\psi(z)$ is a function of depth and is represented by

$$\psi(z) = \frac{p+2}{p+2-s}\left(1 - s\left(\frac{z}{H}\right)^{p+1}\right) \tag{7},$$

which is related to the function determined empirically by Whillans (1979). In expression (7) z represents the depth in the glacier, H the total thickness of the glacier, s is a constant chosen to be 1 for no bottom sliding, and p is a constant that determines the shape of the velocity profile through the glacier. The computer program listed in Appendix C uses p equal to 1, and Figure 6 shows how hypothetical velocity profiles look for p=1 and p=3. Factor $\psi(z)$ is largest at the surface of the glacier and zero at its base.

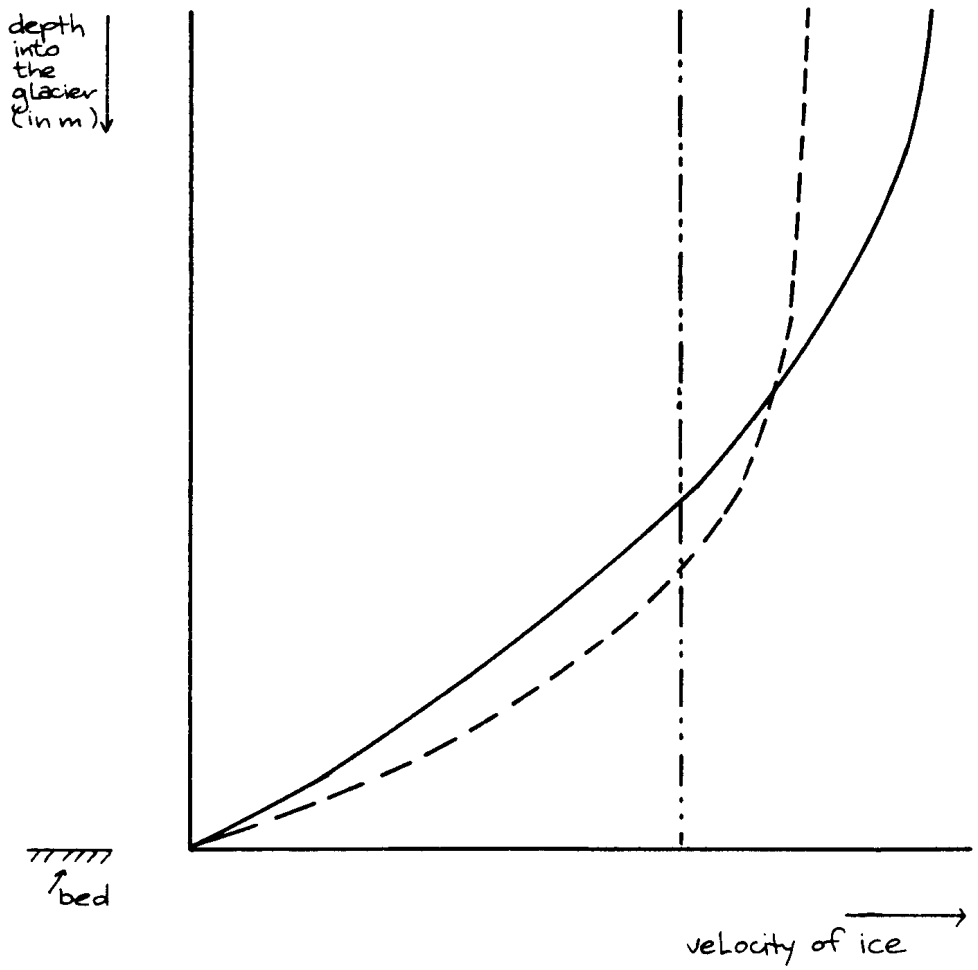

Figure 6. Hypothetical velocity profiles for p=1 and p=3.

———:velocity profile for p=1
– – –:velocity profile for p=3
–·–·—:average velocity for both p=1 and p=3

Combining the effects of thinning of ice above the particle due to compressive vertical strain rates, and of the thickness of the ice layer added by accumulating snow:

$$dz = z \frac{\bar{\dot{\varepsilon}}_z}{\bar{u}_x} dx + \frac{\dot{b}}{\bar{u}_x \psi(z)} dx. \tag{8}$$

In fact, this expression is valid anywhere along the glacier. Mass balance $\dot{b}$ ($\dot{b}_{ac}$ in the accumulation zone and $-\dot{b}_{ab}$ in the ablation zone) and mean vertical strain rate $\bar{\dot{\varepsilon}}_z$ in general have signs opposite in the ablation zone from the accumulation zone, because in the ablation zone ice ablates instead of accumulates and vertical strain rates are usually tensile instead of compressive. This causes a particle to move downward through the glacier in the accumulation zone, and upward in the ablation zone.

Dividing each side of equation (8) by dx, and attaching function-variable x to the appropriate variables, the change in depth of a particle is described by the differential equation:

$$\frac{dz}{dx} = z(x) \frac{\bar{\dot{\varepsilon}}_z(x)}{\bar{u}_x(x)} + \frac{\dot{b}(x)}{\bar{u}_x(x)\psi(z)}. \tag{9}$$

This enables one to find the depth in the glacier of a particle, at various distances from the snout, if ice thickness z(x), mean vertical strain rate $\bar{\dot{\varepsilon}}_z(x)$, mean velocity in the x-direction $\bar{u}_x(x)$, and mass balance $\dot{b}(x)$ are known.

In Appendix B, a finite-difference approximation is developed for equation (9). This is used to calculate particle trajectories through the glacier. An age calculation is made simultaneously. A particle that is buried in the accumulation zone travels along a flowline to the ablation zone (see Figure 5). The time it takes this particle to travel

along the flowline determines how old it is when it reappears in the ablation zone near the Allan Hills.

As noted before, time elapsed dt equals $dx/\bar{u}_x\psi(z)$, where dx is the distance travelled and $\bar{u}_x\psi(z)$ the velocity in the x-direction of the particle at depth z. To find the total time travelled by the particle, each period of time dt it takes to travel a distance dx is added.

The particle with the longest trajectory has also been buried deepest in the glacier (see Figure 5). Deep in the glacier $\psi(z)$, and consequently $u_x(z)$, approaches zero. Therefore, the particle that is buried the deepest also travels the slowest. As a result, ice that has travelled along a long trajectory before reappearance in the ablation zone is even older than its long trajectory may suggest. As seen in Figure 5, this means that ice closest to the Allan Hills is oldest and becomes younger towards the equilibrium line.

In summary, the depth equation derived above is used to calculate particle trajectories and ages of ice near the Allan Hills. The calculations are performed in the computer program listed in Appendix C, which is the same program in which meteorite concentrations are calculated.

CHAPTER FOUR

SENSITIVITY OF RESULTS TO INPUT PARAMETERS

Chapters 2 and 3 describe how the meteorite concentration and age of the ice at the surface of the Allan Hills are calculated. The calculations are performed in the computer program listed in Appendix C and uses parameters suggested by Whillans and Cassidy (in press). This chapter demonstrates how varying those parameters influences the number of meteorites and age of the ice calculated.

Results using the values suggested by Whillans and Cassidy (in press) are regarded as standard. Parameters are changed, one at the time, and the results are shown in Table 1. The remainder of this chapter discusses the importance of each parameter.

4.1 Exponent 1/Q in the thickness equation ((10a) and (10b), Chapter 2).

When 1/Q is decreased from .75 to .7, the maximum thickness of the glacier decreases by 44%. This means that the cross-sectional area perpendicular to the flow direction decreases. Because the ablation rate ($\dot{b}_{ab}$) and accumulation rate ($\dot{b}_{ac}$) are maintained at the same level, the ice flux remains the same and the ice flows faster to compensate for the loss in cross-sectional area. The average increase in surface velocity is 77%.

The change in exponent 1/Q does not change the positions where ice flow trajectories end and start, but it does change the maximum depth of the trajectories. In both the standard and altered program, the deepest trajectories reach a depth of 55% of the maximum thickness of the

PARAMETER SYMBOL AND MEANING	ORIGINAL PARAMETER VALUE	NEW PARAMETER VALUE	PERCENTAGE CHANGE IN PARAMETER VALUE	PERCENTAGE CHANGE IN METEORITE CONCENTRATION — 21000m. FROM SNOUT	PERCENTAGE CHANGE IN METEORITE CONCENTRATION — 81000 m. FROM SNOUT	PERCENTAGE CHANGE IN AGE OF ICE — 21000m FROM SNOUT	PERCENTAGE CHANGE IN AGE OF ICE — 81000 m. FROM SNOUT
$\dot{b}_{ac}$ (accumulation rate)	.039 m/a	.03939 m/a	1	-.48	-.56	-.58	.03
$\dot{b}_{ac}$	.039 m/a	.0468 m/a	20	-9.98	-10.07	-11.70	-7.38
$\dot{b}_{ab}$ (ablation rate)	.06 m/a	.0606 m/a	1	-.24	-.42	-.30	-.47
$\dot{b}_{ab}$	.06 m/a	.0720 m/a	20	-6.41	-6.57	-6.35	-8.09
f (meteorite infall rate)	60×10^{-12} kg/m²a	72×10^{-12} kg/m²a	20	19.95	20.00	.06	.38
f	60×10^{-12} kg/m²a	60.6×10^{-12} kg/m²a	1	.95	.98	.05	.31
p (part of exponent in ψ-eqn)	1	2	100	12.59	12.59	3.92	12.35
p	1	3	200	19.95	20.00	6.75	20.84
a (coefficient thickness equation)	.6	.5	-16.67	-16.63	-16.64	-16.61	-16.59
a	.6	.606	1	.95	.98	.99	.75
$1/Q$ (exponent thickness equation)	.75	.7575	1	7.84	8.81	10.99	9.06
$1/Q$	.75	.7000	-6.67	-39.19	-43.22	-42.37	-43.65
R (measure of flowline spreading $\frac{dR}{dz} \to \infty$, // flow)	100,000 m.	120,000 m.	20	8.08	9.65	7.90	10.32
R	100,000 m.	101,000 m.	1	.48	.56	2.11	.59
$\dot{z}$ (thickness change of glacier)	0 m/a	.001 m/a		-2.14	-1.68	-2.44	-1.64
$\dot{z}$	0 m/a	.002 m/a		-4.28	-3.36	-8.82	-3.56
X_{EQ} (position equilibrium line)	101,000 m	91,000 m	-9.9	-34.20	-47.83	-7.82	-53.22
X_{EQ}	101,000 m	71,000 m	-29.7	-28.27	This position is no longer in the ablation zone	-30.70	This position is no longer in the ablation zone

Table 1. Effect of parameter changes on meteorite concentration and age of ice.

glacier. Because the thickness of the glacier in the altered program is smaller, its deepest trajectory reaches a shallower depth than that in the standard program. As a result, trajectories are shorter and this combined with the faster travel time causes the age of the ice to be much smaller (about 43% all along the ablation zone).

A decrease in 1/Q also results in an increase in the absolute value of the sum of the horizontal strain rates in the ablation zone. Therefore, meteorites that reach the surface of the ablation zone become more crowded, and these crowded meteorites are transported faster to the snout, because surface velocities along the ablation zone are higher. As a result, meteorites collect in large numbers at the snout (possibly in an end moraine) and concentrations at the surface of the ablation zone are lower than those found in the standard program (about 41% lower all along the ablation zone).

The results discussed above are exactly opposite if exponent 1/Q is increased instead of decreased. Changing this exponent has a very significant effect on both the meteorite concentration and age of the ice, because it changes the thickness of the glacier.

4.2 Position of the equilibrium line x_{eq}.

When the position of the equilibrium line is closer to the glacier snout, the size of the ablation zone is decreased. This means that the area where meteorites collect is smaller, so that the third meteorite concentrating mechanism, which crowds meteorites once they are on the surface of the ablation zone (see Chapter 2), cannot work as effectively. Therefore, the meteorites are crowded to a lesser extent and smaller meteorite concentrations are found.

In addition, velocities and trajectory lengths decrease. The decrease in velocities may be expected to lead to an increase in the age of the ice near the Allan Hills. This does not happen, however, because the shorter path of travel of the emerging ice is more important.

4.3 Accumulation rate $\dot{b}_{ac}$.

An increase in the accumulation rate decreases the concentration of meteorites within the glacier. Therefore, the concentration of meteorites at the surface of the ablation zone is also smaller, because relatively less meteorites are supplied by the glacier.

The increase in $\dot{b}_{ac}$ causes a decrease in velocities. In spite of this, ages of the ice decrease, because trajectories are shorter.

4.4 Ablation rate $\dot{b}_{ab}$.

An increase in the ablation rate causes an increase in velocities all along the glacier, if the glacier stays in steady state condition. The higher rate of ice removal is compensated by a higher rate of ice supply. This causes particles to move faster along their trajectories, and consequently ages of the ice decrease.

In addition, horizontal surface strain rates are more negative, which would lead to greater meteorite concentrations, but the higher surface velocities in the ablation zone result in smaller meteorite concentrations as described in section 4.1.

4.5 Meteorite infall rate f.

If f is increased by a certain percentage, the meteorite concentration in the ablation zone increases by the same percentage. This parameter has no influence on the age of the ice.

4.6 Constant p in the ψ-equation ((7), Chapter 3).

As described in Chapter 3, an increase in p does not change the mean velocity and strain rate through the glacier, but it does decrease the velocity and strain rate at and near the surface and increases them at depth. When horizontal surface strain rates become less negative, meteorites at the surface of the ablation zone become less crowded, and smaller surface velocities cause these less crowded meteorites to remain at the glacier surface longer. As a result, an increase in p causes an increase in the meteorite concentration at the surface in the ablation zone.

An increase in p leads to slower velocities near the surface, so that ice which travels along shallow trajectories is older when it reaches the surface in the ablation zone. A deep trajectory passes through shallow and deep regions both. As a result, the age of ice that has travelled along such a trajectory depends on whether the deep part of the trajectory is long compared with the shallow part, because velocities are larger at increased depths for a larger value of p.

This means that ice that emerges near the glacier snout and has travelled along deep trajectories, can be older or younger when p is increased, depending on the length of the trajectory. Even if this ice is older, its relative increase in age will be less than that of ice that has been buried at shallow depths and emerges close to the equilibrium line.

4.7 Coefficient "a" in the thickness equation ((10a) and (10b), Chapter 2).

The maximum ice thickness decreases in proportion to "a". Thus, for the same reasons as described in section 4.1, smaller concentrations

of meteorites and ages of ice are expected at the surface of the ablation zone.

4.8 Radius of curvature of ice elevation contours R.

This parameter is a measure of the divergence of ice flow. The larger R, the less divergent is the ice flow, because R is the radius of curvature of ice elevation contours and ice flows perpendicular to these contours. R is used in Appendix A to approximate lateral surface strain rate $\dot{\varepsilon}_{sy}$.

If R is increased, velocities decrease all along the glacier, and the absolute value of the horizontal surface strain rates increases. This results in higher meteorite concentrations, as explained in Section 4.1.

The smaller velocities result in the emergence of older ice at the surface of the ablation zone.

4.9 Rate of ice thickness change $\dot{z}$.

The equations of the model developed in Chapters 2 and 3 partly allow for non-steady flow through $\dot{z}$. A more correct calculation for non-steady state conditions would include a more careful solution of the continuity equation for velocity. Nevertheless, some idea of non-steady effects can be obtained from the equations as used in this report.

An increase in $\dot{z}$ (that is, past thickening of the glacier), causes an increase of velocities and absolute values of the sum of the horizontal strain rates all along the glacier. As described in section 4.1, this means that less meteorites and younger ice are found at the surface in the ablation zone.

4.10 Summary

The discussions above show that large concentrations of meteorites and old ice are favored if the glacier is thick and velocities are low. In addition, a steep velocity profile, a large ablation area, low ablation rates, low accumulation rates or less divergent ice flow have the same effect. If one or more of these conditions is present, the emergence of old ice in the ablation zone near the Allan Hills and the accumulation of meteorites in large numbers is enhanced.

CHAPTER FIVE

CONCLUSIONS

The model developed in this report explains why meteorites and old ice are found at the surface in the ablation zone of the Allan Hills, and enables one to calculate expected meteorite concentrations and ages of the ice. This model is applicable in any other location where conditions are similar to those near the Allan Hills.

To find new meteorite collecting sites and locations where old ice emerges, one should look for an ablation zone near mountains that obstruct the glacial flow. These mountains do not have to rise above the ice surface, but can be overlain by a relatively thin layer of ice. If that is the case, ice flow is still obstructed significantly enough to ensure upward flow in the ablation zone, thus exposing new meteorites and old ice.

The largest numbers of meteorites and oldest ice are to be found if the glacier is thick and flows at low velocities with little divergence. In addition, a large ablation area with small ablation rates, steep velocity profiles and small accumulation rates in the source area of the ice are conditions that favor the presence of large concentrations of meteorites and old ice.

ADDENDUM

In Chapter 3 an error is made in deriving depth equation (9). As described, the depth of a particle in the glacier changes because the length of the ice column above it changes due to compressive vertical strain rates. In addition, its depth also changes because snow is added above the column during time dt. The thickness of the layer of snow added is expressed in Chapter 3 as

$$z' = \frac{\dot{b}_{ac}\,dx}{\bar{u}_x \psi(z)},$$

because dt is substituted by $dx/\bar{u}_x\psi(z)$, where $\bar{u}_x\psi(z)$ is the velocity at depth z. This substitution in incorrect. Time interval dt should have been replaced by dx/u_{sx}, where u_{sx} is the velocity of the ice at the surface of the glacier. Therefore, equation (6) in Chapter 3 becomes

$$z' = \frac{\dot{b}_{ac}\,dx}{u_{sx}},$$

and depth equation (9)

$$\frac{dz}{dx} = z(x)\,\frac{\bar{\dot{\varepsilon}}_z(x)}{\bar{u}_x(x)} + \frac{\dot{b}(x)}{u_{sx}(x)}.$$

As a result, the solution to the revised depth equation (see Appendix B) is

$$z_{new} = z_{old}\,\exp\left(\frac{\bar{\dot{\varepsilon}}_z \Delta x}{\bar{u}_x}\right) + \frac{\dot{b}}{\dot{\varepsilon}_{sz}}\left(\exp\left(\frac{\bar{\dot{\varepsilon}}_z \Delta x}{\bar{u}_x}\right) - 1\right),$$

where $\dot{\varepsilon}_{sz}$ is the vertical strain rate at the surface.

The error means that the values calculated by the computer program in Appendix C are off by some factor. In spite of this, the interpretations in Chapter 4 remain the same. The different values calculated will only change the entries of Table 1 (Chapter 4) and the positions of the graphs in Appendix D. The shapes of these graphs remain the same.

REFERENCES

Cassidy, W.A., Olsen, E., and Yanai, K. 1977. Antarctica: A Deep-Freeze Storehouse for Meteorites. Science, Vol. 198, p. 727-31.

_____, and Rancitelli, L.A. 1982. Antarctic Meteorites. Am. Scientist, Vol. 70, p. 156-64.

Drewry, D.J. 1975. Radio Echo Sounding Map of Antarctica, (90°E - 180°). Polar Record, Vol. 17, No. 109, p. 359-74.

_____ 1977. Ice Flow, Bedrock, and Geothermal Studies from Radio-Echo Sounding Inland of McMurdo Sound, Antarctica. Ant. Geoscience (ed. Craddock, C.) (Univ. of Wisconsin Press), p. 977-83.

Fireman, E.L., Norris, T.L. 1982. Ages and Composition of Gas trapped in Allan Hills and Byrd Core Ice. Earth and Planet. Sci. Lett., Vol. 60, p. 339-50.

Nagata, T. 1978. A Possible Mechanism of Concentration of Meteorites within the Meteorite Ice Field in Antarctica. Mem. Natl. Inst. Polar Res., Spec. Issue 8, p. 70-92.

Nishiizumi, K., Arnold, J.R., Elmore, D., Ferraro, R.D., Gove, H.E., Finkel, R.C., Beukens, R.P., Chang, K.H., and Kilius, L.R. 1979. Measurements of ^{36}Cl in Antarctic Meteorites and Antarctic Ice using a Van de Graaff Accelerator. Earth and Planet. Sci. Lett., Vol. 45, p. 285-92.

_____, Murrell, M.T., Arnold, J.R., Elmore, D., Ferraro, R.D., Gove, H.E., and Finkel, R.C. 1981. Cosmic-ray-produced ^{36}Cl and ^{53}Mn in Allan Hills-77 meteorites. Earth and Planet. Sci. Lett., Vol. 52, p. 31-38.

Nishio, F., and Annexstad, J.O. 1980. Studies on the Ice Flow in the Bare Ice Area near the Allan Hills in Victoria Land, Antarctica. Mem. Natl. Inst. Polar Res., Spec. Issue 17, p. 1-13.

_____, Azuma, N., Higashi, A., and Annexstad, J.O. 1982. Structural Studies of Bare Ice near the Allan Hills, Victoria Land, Antarctica: A Mechanism of Meteorite Concentration. Annals of Glaciology, Vol. 3, p. 222-226.

Paterson, W.S.B. 1981. The Physics of Glaciers. Oxford. Pergamon Press, 380 p.

Whillans, I.M. 1977. The Equation of Continuity and its Application to the Ice Sheet near "Byrd" Station, Antarctica. J. of Glaciology, Vol. 18, No. 80, p. 359-71.

Whillans, I.M. 1979. Ice flow along the Byrd Station Strain Network, Antarctica. J. of Glaciology, Vol. 24, No. 90, p. 15-28.

_____, and Cassidy, W.A. Catch a Falling Star: Meteorites and Old Ice. Science, in press.

Yanai, K. 1978. First Meteorites Found in Victoria Land, Antarctica, December 1976 and January 1977. Mem. Natl. Inst. Polar Res., Spec. Issue 8, p. 51-69.

Yoshida, M., Ando, H., Omoto, K., Naruse, R., and Ageta, Y. 1971. Ant. Record, Vol. 39, p. 62-65.

APPENDIX A

Explanations for substitutions in equations

A1. Explanation for the substition $\dot{\varepsilon}_{sy} = \frac{|u_{sx}|}{R}$

In Chapter 2 on page 10 lateral surface strain rate, $\dot{\varepsilon}_{sy}(x)$, is substituted by $\frac{|u_{sx}(x)|}{R}$, where $|u_{sx}(x)|$ is the absolute value of the surface velocity in the x-direction, and R is the radius of curvature of the elevation contours.

Figure 7 shows a map view of some part of the glacier near the Allan Hills. Curve S represents an ice surface elevation contour. It is assumed this elevation contour is part of a circle with radius R.

Ice flows perpendicular to elevation contours. Therefore, vectors $\vec{AB}$ and $\vec{CD}$ represent surface velocity vectors of ice at positions A and C respectively. In the limit, as Δy approaches zero, vector $\vec{CD}$ can be approximated by $C'D$, and the x-component of this vector by $-\vec{u}_{sx}$. The component in the y-direction is represented by $\vec{u}_{sy}$.

Lateral surface strain rate, $\dot{\varepsilon}_{sy}$, is defined as the change in surface velocity in the y-direction divided by the distance over which this change occurs (Paterson, 1981, p. 65). Figure 7 shows that the change in surface velocity in the y-direction equals $\vec{u}_{sy}$ and Δy is the distance over which this change occurs. Therefore, lateral strain rate $\dot{\varepsilon}_{sy}$ equals $\frac{\vec{u}_{sy}}{\Delta y}$.

Triangles EAC' and C'FD are similar triangles, so that by geometry $\frac{\vec{u}_{sy}}{\Delta y}$ equals $\frac{-\vec{u}_{sx}}{R}$. In this project the direction of the positive x-axis is opposite to the direction of ice flow, such that $-\vec{u}_{sx}$ is always positive. Therefore, the lateral surface strain rate $\dot{\varepsilon}_{sy}$ can be approximated by the absolute value of the surface velocity in the x-direction divided by the

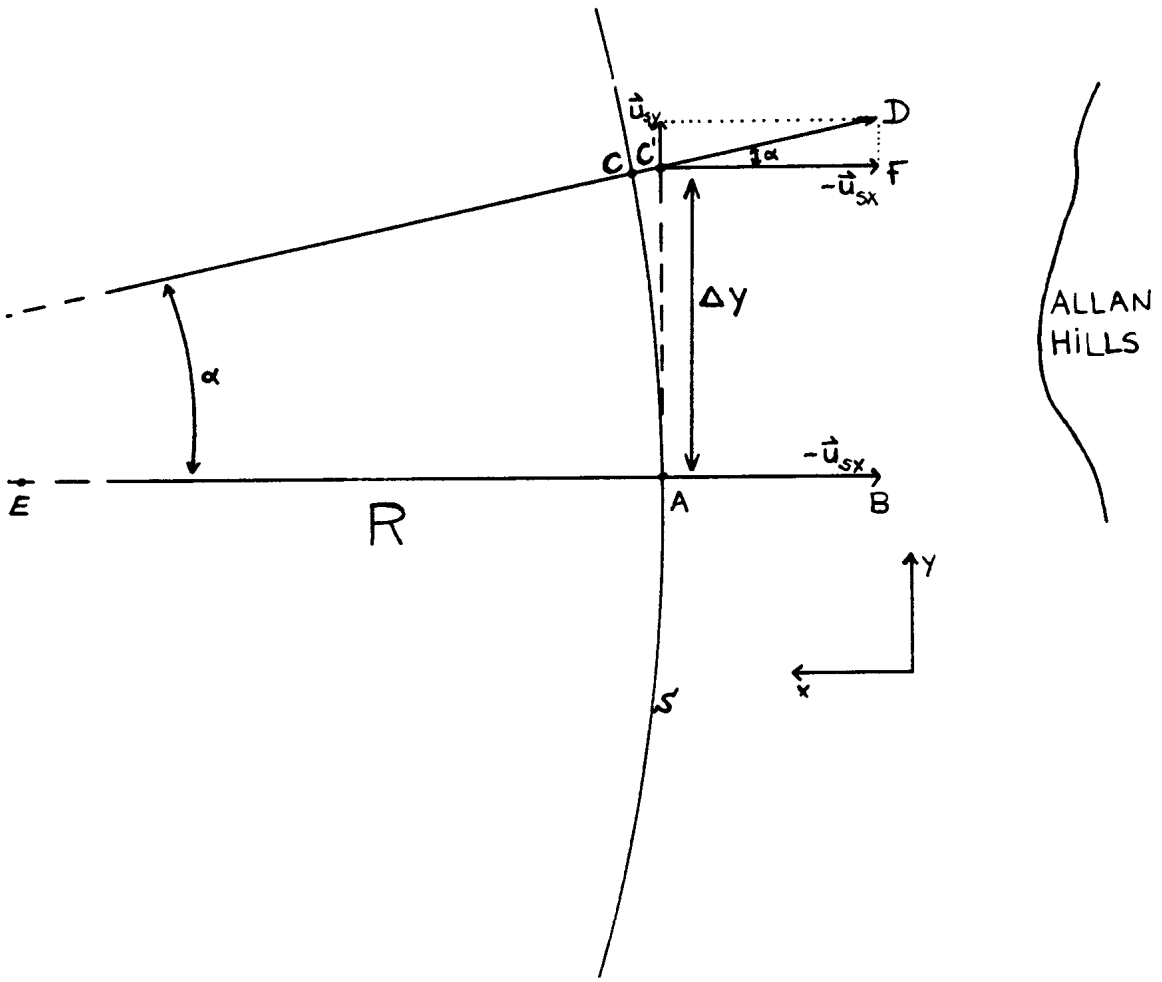

Figure 7. Map view of the glacier near the Allan Hills. S is an ice elevation contour and $\vec{AB}$ and $\vec{CD}$ are velocity vectors of ice at positions A and C respectively.

radius of curvature: $\dot{\varepsilon}_{sy} = \frac{|u_{sx}|}{R}$.

A2. Substitution of partial derivative $\frac{\partial z(x)}{\partial x}$

The change in thickness of the glacier with distance is expressed as $\frac{\partial z(x)}{\partial x}$, and is derived from equations (10a) and (10b) in Chapter 2. Equation (10a) is

$$z(x) = ax^{1/Q} - \dot{z}(t_o - t) \text{ for } x \leq x_{eq}$$

and equation (10b) is

$$z(x) = a\, x_{eq}^{1/Q} - \dot{z}(t_o - t) \text{ for } x \geq x_{eq}.$$

Therefore, the partial derivative of z with respect to x is

$$\frac{\partial z(x)}{\partial x} = \frac{a}{Q} x^{1/Q-1} \quad \text{for } x \leq x_{eq}$$

and

$$\frac{\partial z(x)}{\partial x} = 0 \quad \text{for } x \geq x_{eq}.$$

Term $\frac{\partial z(x)}{\partial x}$ is zero in the accumulation zone, because there the thickness is taken to be constant.

For steady state ($\dot{z}$=0), thickness z(x) in the ablation zone is expressed as $ax^{1/Q}$. This means that there $\frac{1}{z(x)} \frac{\partial z(x)}{\partial x}$ equals $\frac{1}{Qx}$.

The equalities described above are substituted into expression (14) of Chapter 2, which is an expression for the sum of the horizontal surface strain rates. For calculations performed in the computer program listed in Appendix C this new version of expression (14) is used, which is

$$\dot{\varepsilon}_{sx,sy}(x) = \frac{-u_{sx}(x)}{Qx} + \frac{(\dot{b}(x) - \dot{z})\psi(o)}{z(x)}$$

for positions in the ablation zone and

$$\dot{\varepsilon}_{sx,sy}(x) = \frac{1}{z(x)} \left\{(\dot{b}(x) - \dot{z})\psi(o)\right\}$$

for positions in the accumulation zone.

APPENDIX B

Conversion of differential equations

for finite differencing

B1. Conversion of the equation for u_{sx}, the ice surface velocity in the in the x-direction

Equation (9) in Chapter 2 states that the surface velocity in the x-direction is:

$$u_{sx} = \frac{1}{z} \int_{o}^{x} \left\{ (\dot{b} - \dot{z})\psi(o) - z\dot{\varepsilon}_{sy} \right\} \partial x.$$

This expression shows that the ice flux at a certain position along the x-axis ($u_{sx}z$) can be expressed as:

$$u_{sx}\, z = \int_{o}^{x} \left\{ (\dot{b} - \dot{z})\psi(o) - z\, \dot{\varepsilon}_{sy} \right\} \partial x \qquad (1).$$

Equation (1) is a differential equation that is approximated so it can be used in the calculations of the computer program listed in Appendix C.

The right hand side (RHS) of expression (1) represents the sum of all the fluxes through the glacier between positions 0 and x along the x-axis. If infinitely small distance step ∂x is replaced by somewhat larger distance step Δx, the RHS of expression (1) can be simplified, so that the whole expression becomes:

$$(u_{sx}z)_{\text{new total}} = \left\{ (\dot{b} - \dot{z})\psi(o) - z\, \dot{\varepsilon}_{sy} \right\} \Delta x + (u_{sx}z)_{\text{old total}} \qquad (2).$$

To find the surface velocity at the new position, the new total flux $u_{sx}z$ is divided by the thickness of the glacier (z) at the new position. Equation (2) is suitable for use in a computer program.

Using distance step Δx instead of ∂x in the calculations causes inaccuracies. To limit the size of these inaccuracies, average values are used for parameters over distance interval Δx.

Calculations are made along the glacier in the direction of the positive x-axis (see Figure 8), and the parameters used and values to be calculated at the new position are indicated by a prime symbol. When averaging procedures are introduced in expression (2), and lateral surface strain rate $-\dot{\varepsilon}_{sy}$ is substituted by $\frac{u_{sx}}{R}$ (see Appendix A), this expression can be written as:

$$z'u_{sx}' = \left\{\left(\frac{\dot{b} + \dot{b}'}{2} - \frac{\dot{z} + \dot{z}'}{2}\right)\psi(o) + \left(\frac{z + z'}{2}\right)\left(\frac{u_{sx} + u_{sx}'}{2}\right)/R\right\}\Delta x + zu_{sx}$$

which reduces to:

$$z'u_{sx}' = \left\{\left[\left(\frac{\dot{b} + \dot{b}'}{2} - \dot{z}\right)\psi(o) + \frac{u_{sx}}{4R}(z + z')\right]\Delta x + zu_{sx}\right\}/\left\{1 - \frac{\Delta x}{4R}\left(\frac{z}{z'} + 1\right)\right\} \quad (3).$$

Expression (3) is used in the computer program listed in Appendix C and from it, the surface velocity in the x-direction, u_{sx}, is found.

B2. Conversion of the equation for M, the meteorite concentration along the surface of the glacier.

Expression (2) in Chapter 2 is the differential equation:

$$\frac{dM}{dx} = \left(\frac{f}{\dot{b}_{ac}}\dot{b}_{ab} + f - \dot{\varepsilon}_{sx,sy}M\right)/u_{sx}.$$

If both sides of this equation are multiplied by dx, and if dx and dM are replaced by Δx and ΔM respectively, the equation becomes:

$$\Delta M = \left(\frac{f}{\dot{b}_{ac}}\dot{b}_{ab} + f - \dot{\varepsilon}_{sx,sy}M\right)\frac{\Delta x}{u_{sx}}. \quad (4)$$

By definition the change in meteorite concentration ΔM equals the new meteorite concentration, M_{new}, minus the old meteorite concentration, M_{old}. Similarily distance step Δx equals $x_{new} - x_{old}$. The calculation to find the meteorite concentration along the ablation surface, however, starts at the equilibrium line, which is in the direction of the negative x-axis. This means that distance step Δx has a negative value.

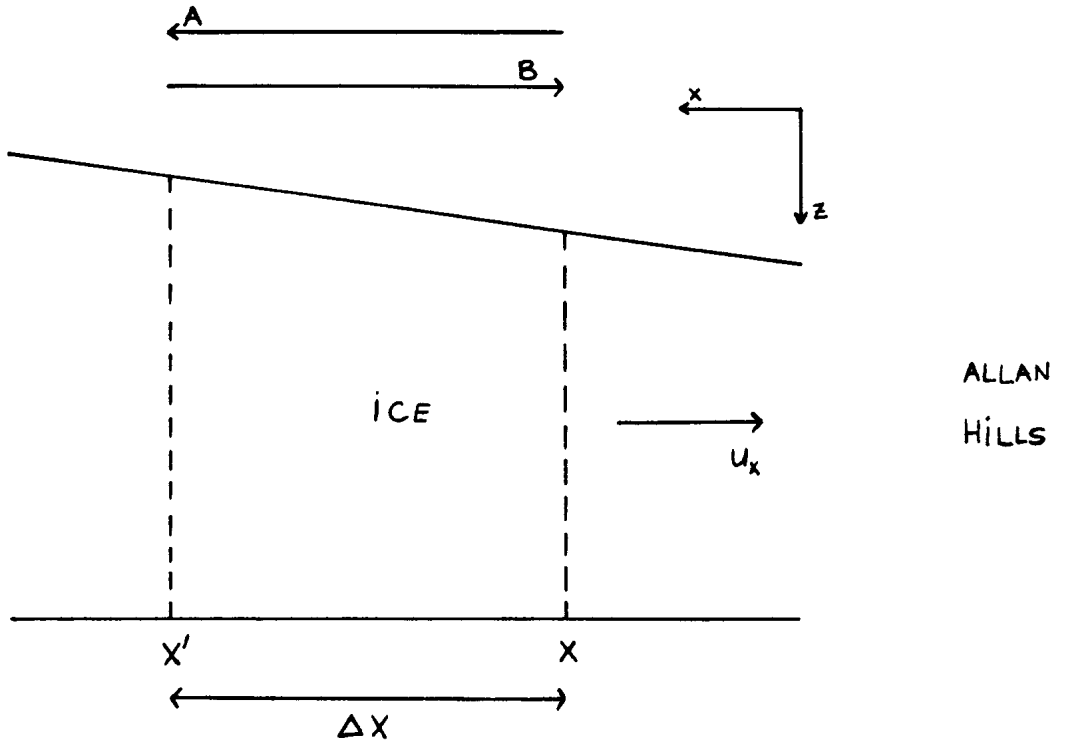

Figure 8. Profile of the glacier near the Allan Hills. The prime position is located farthest from the glacier snout. Arrow A indicates the direction of calculation for the expressions described in sections B1 and B3. Arrow B indicates the direction of calculation for the expression described in Section B2.

The equalities described above are substituted into expression (4), which results in

$$M_{new} = \left(\frac{f}{\dot{b}_{ac}}\,\dot{b}_{ab} + f - \dot{\varepsilon}_{sx,sy}M\right)\frac{\Delta x}{u_{sx}} + M_{old} \qquad (5),$$

and is the finite differenced form of expression (2) in Chapter 2.

As in the former section, using distance step Δx in the calculations, instead of dx, causes inaccuracies. Again average values over distance interval Δx are used for those parameters for which the averaging procedures are relevant.

This means (from figure 8) that equation (5) can be expressed as

$$M = \left\{\frac{f}{\dot{b}_{ac}}\,\dot{b}_{ab} + f - \frac{(\dot{\varepsilon}_{sx,sy} + \dot{\varepsilon}_{sx,sy'})}{2}\frac{(M + M')}{2}\right\}\Delta x \Big/ \frac{(u_{sx} + u_{sx'})}{2} + M'$$

which reduces to

$$M = \left\{\left(\frac{f}{\dot{b}_{ac}}\,\dot{b}_{ab} + f - \frac{(\dot{\varepsilon}_{sx,sy} + \dot{\varepsilon}_{sx,sy'})}{4}\,M'\right)\frac{2\Delta x}{(u_{sx} + u_{sx'})} + M'\right\} \Big/$$

$$\left\{1 - \frac{(\dot{\varepsilon}_{sx,sy} + \dot{\varepsilon}_{sx,sy'})\Delta x}{(u_{sx} + u_{sx'})\,2}\right\} \qquad (6).$$

Expression (6) is used in the computer program listed in Appendix C and from it, meteorite concentrations (M) at various positions along the ablation zone are found.

B3. Conversion of the depth equation, (9), in Chapter 3.

The depth equation derived in Chapter 3 is:

$$\frac{dz}{dx} = z\,\frac{\bar{\dot{\varepsilon}}_z}{\bar{u}_x} + \frac{\dot{b}}{\bar{u}_x \psi(z)}\,.$$

A solution to this differential equation is

$$z_{new} = z_{old} \exp\left(\frac{\bar{\dot{\varepsilon}}_z \Delta x}{\bar{u}_x}\right) + \frac{\dot{b}}{\psi(z)\bar{\dot{\varepsilon}}_z}\left(\exp\left(\frac{\bar{\dot{\varepsilon}}_z \Delta x}{\bar{u}_x}\right) - 1\right) \qquad (7),$$

if Δx is a small distance step. This solution is used to calculate ice flow trajectories.

As explained earlier, average values over interval Δx should be used for the parameters in equation 7 to minimize inaccuracies in the calculations. Because calculations using the depth equation are made in the positive x-direction (see Figure 8), expression (7) is written as:

$$z' = z \exp\left(\frac{(\dot{\varepsilon}_z + \dot{\varepsilon}_z')\Delta x/2}{(\bar{u}_x + \bar{u}_x')/2}\right) + \left(\frac{(\dot{b}+\dot{b}')/2}{\{(\psi(z)+\psi(z'))/2\}\{(\bar{\dot{\varepsilon}}_z + \bar{\dot{\varepsilon}}_z')/2\}}\right)\left(\exp\left(\frac{(\bar{\dot{\varepsilon}}_z + \bar{\dot{\varepsilon}}_z')\Delta x/2}{(\bar{u}_x + \bar{u}_x')/2}\right) - 1\right),$$

which simplifies to

$$z' = z \exp\left(\frac{(\bar{\dot{\varepsilon}}_z + \bar{\dot{\varepsilon}}_z')\Delta x}{(\bar{u}_x + \bar{u}_x')}\right) + \left(\frac{(\dot{b}+\dot{b}')/2}{(\psi(z)+\psi(z'))(\bar{\dot{\varepsilon}}_z + \bar{\dot{\varepsilon}}_z')}\right)\left(\exp\left(\frac{(\bar{\dot{\varepsilon}}_z + \bar{\dot{\varepsilon}}_z')\Delta x}{(\bar{u}_x + \bar{u}_x')}\right) - 1\right) \qquad (8).$$

Expression (8) is used to calculate particle trajectories in the program listed in Appendix C. Term $\psi(z')$ is never found exactly, because in order to find it the new depth, which is to be calculated, must be known. The term is approximated by a variable called DUMMY. In DO-loop 8 of the program, DUMMY is recalculated many times until it is very close to the true value of $\psi(z')$.

APPENDIX C

Fortran Program

PROGRAM SUMMARY:

Between A and B: variables are calculated for the ablation zone.

Between B and C: particle trajectories and travel times are calculated.

Between C and D: meteorite concentrations along the surface in the ablation zone are calculated.

```
C*****************************************************************C
C**                                                             **C
C**   MEANING OF VARIABLES                                      **C
C**                                                             **C
C**   A       = COEFFICIENT OF THICKNESS EQUATION               **C
C**   AB      = ABLATION RATE IN METERS PER YEAR                **C
C**   ABL     = ABLATION RATE IN METERS PER YEAR                **C
C**   AC      = ACCUMULATION RATE IN METERS PER YEAR            **C
C**   ANEWZ$  = THICKNESS GLACIER AT X IN METERS                **C
C**   BDOT    = ACCUMULATION RATE IN METERS PER YEAR            **C
C**   BDOTN   = ABLATION RATE IN METERS PER YEAR                **C
C**   CONCTN  = METEORITE CONCENTRATION AT X IN KILOGRAM        **C
C**             PER METERS SQUARED                              **C
C**   CORFAC  = VARIABLE (PSI IN TEXT) THAT RELATES MEAN        **C
C**             AND SURFACE VALUES FOR STRAIN RATE AND          **C
C**             VELOCITY                                        **C
C**   DELTAX  = DISTANCE STEP IN METERS                         **C
C**   DEPTH   = DEPTH OF A PARTICLE IN METERS                   **C
C**   DUMMY   = TEMPORARY CORFAC                                **C
C**   ESNZMN  = MEAN VERTICAL STRAIN RATE AT X IN PER           **C
C**             YEAR                                            **C
C**   ESNZTP  = MEAN VERTICAL STRAIN RATE AT X IN PER           **C
C**             YEAR                                            **C
C**   ESNX$Y  = SUM OF HORIZONTAL SURFACE STRAIN RATES IN       **C
C**             PER YEAR                                        **C
C**   EXPONT  = EXPONENT IN DEPTH EQUATION                      **C
C**   F       = METEORITE INFALL RATE IN KILOGRAM PER           **C
C**             METERS SQUARED PER YEAR                         **C
C**   I       = COUNTER                                         **C
C**   IP      = POSITION INDICATOR                              **C
C**   J       = COUNTER                                         **C
C**   K       = COUNTER                                         **C
C**   K       = POSITION INDICATOR                              **C
C**   KL      = COUNTER                                         **C
C**   KLK     = POSITION INDICATOR                              **C
C**   KM      = COUNTER                                         **C
C**   KZ      = POSITION INDICATOR                              **C
C**   L       = POSITION INDICATOR                              **C
C**   LX      = COUNTER                                         **C
C**   M       = POSITION INDICATOR                              **C
C**   MN      = COUNTER                                         **C
C**   MX      = COUNTER                                         **C
C**   MXM     = POSITION INDICATOR                              **C
C**   MXMX    = POSITION INDICATOR                              **C
C**   N       = CONSTANT (P IN TEXT) FOR CORFAC- EQUATION       **C
C**   NX      = POSITION INDICATOR                              **C
C**   NXP     = POSITION INDICATOR                              **C
C**   PHI     = VALUE OF CORFAC FOR Z=0                         **C
C**   Q       = RECIPROCAL OF EXPONENT OF THICKNESS             **C
C**             EQUATION                                        **C
C**   R       = RADIUS OF CURVATURE OF ICE ELEVATION            **C
C**             CONTOURS IN METERS                              **C
C**   RX      = RADIUS OF CURVATURE OF ICE ELEVATION            **C
C**             CONTOURS IN METERS                              **C
C**   TIME    = TIME IN YEARS                                   **C
C**   TNEW    = TOTAL TIME IN YEARS                             **C
C**   TOLD    = TOTAL TIME OF FORMER STEPS IN YEARS             **C
C**   TORIG   = INITIAL ESTIMATE FOR TNEW IN YEARS              **C
C**   TXT     = ROUGH ESTIMATE FOR TIME IN YEARS                **C
C**   TZERO   = TIME AT WHICH CALCULATION STARTS IN YEARS       **C
C**   UMEAN   = MEAN VELOCITY AT X IN METERS PER YEAR           **C
C**   US      = SURFACE VELOCITY IN X-DIRECTION IN METERS       **C
C**             PER YEAR                                        **C
C**   US$     = SURFACE VELOCITY IN X-DIRECTION IN METERS       **C
C**             PER YEAR                                        **C
C**   USZ     = FLUX AT X IN METERS SQUARED PER YEAR            **C
C**   USZ$    = FLUX AT X IN METERS SQUARED PER YEAR            **C
C**   USZPR$  = FLUX AT X IN METERS SQUARED PER YEAR            **C
```

```
C**   X       = DISTANCE FROM THE SNOUT IN METERS                    **C
C**   X$      = DISTANCE FROM THE SNOUT IN METERS                    **C
C**   Z       = THICKNESS GLACIER AT X IN METERS                     **C
C**   Z$      = THICKNESS GLACIER AT X IN METERS                     **C
C**   ZDOT    = RATE OF THICKNESS CHANGE IN METERS PER               **C
C**             YEAR                                                 **C
C**   ZO$     = THICKNESS GLACIER AT X IN METERS                     **C
C**   ZPR$    = THICKNESS GLACIER AT X IN METERS                     **C
C**                                                                  **C
C**********************************************************************C
C
      DIMENSION DEPTH(11,101),X(11,101),TIME(11,101),
     >UMEAN(11,101),US(11,101),BDOT(11,101),USZ(11,101),
     >ESNZMN(11,101),ESNZTP(11,101),CORFAC(11,101),Z(11,101)
     >,ESNX$Y(10,12),CONCTN(10,12)
      DATA DELTAX/10000./,A/.6/,Q/1.333333/,TZERO/0./,AB/.06
     >/,RX/100000./,ZDOT/0./,N/1/,F/60.E-12/,AC/.039/
C
C**********************************************************************C
C**                                                                  **C
C**   AAAAAAAAAAAAAAAAAAAAAAAAAAAAAAAAAAAAAAAAAAAAAAAAAAAAAAAAAA   **C
C**   AAAAAAAAAAAAAAAAAAAAAAAAAAAAAAAAAAAAAAAAAAAAAAAAAAAAAAAAAA   **C
C**                                                                  **C
C**********************************************************************C
C
C**   FLUX, SURFACE AND MEAN VELOCITY, AND THICKNESS AT              **C
C**   X=1000 METERS                                                  **C
      PHI=(N+2.)/(N+1.)
      R=RX
      ABL=AB
      US$=0.
      USZ$=0.
      ZO$=0.
      Z$=A*1000.**(1./Q)
      Z(1,2)=Z$
      USZ$=(((US$*(ZO$+Z$))/(4.*R)+PHI*(-ABL-ZDOT))*1000.*
     >USZ$)/(1.-(1000./(4.*R))*(1.+ZO$/Z$))
      USZ(1,2)=USZ$
      US$=USZ$/Z$
      US(1,2)=US$
      UMEAN(1,2)=US(1,2)/PHI
      X(1,2)=1000.
      X$=1000.
      NX=(100000.-DELTAX)/DELTAX
      NXP=NX+1
C**   FLUX, SURFACE AND MEAN VELOCITY, AND THICKNESS AT              **C
C**   X=11000 METERS THROUGH X=101000 METERS AT 10000                **C
C**   METER INTERVALS                                                **C
      DO 5 I=1,NXP
      IF(I.EQ.NX+1) ABL=AB/2.
      ZPR$=A*(X$+DELTAX)**(1./Q)
      USZPR$=(((US$*(Z$+ZPR$))/(4.*R)+PHI*(-ABL-ZDOT))*
     >DELTAX+USZ$)/(1.-(DELTAX/(4.*R))*(1.+Z$/ZPR$))
      US$=USZPR$/ZPR$
      USZ(I+1,I+2)=USZPR$
      US(I+1,I+2)=US$
      UMEAN(I+1,I+2)=US(I+1,I+2)/PHI
      Z(I+1,I+2)=ZPR$
      X(I+1,I+2)=X(I,I+1)+DELTAX
      Z$=ZPR$
      USZ$=USZPR$
      X$=X$+DELTAX
    5 CONTINUE
      ABL=AB
C**   SURFACE AND MEAN VERTICAL STRAIN RATE AT X=1000                **C
C**   METERS                                                         **C
      ANEWZ$=A*1000.**(1./Q)
      ESNZTP(1,2)=US(1,2)/Q/1000.+PHI*(ABL+ZDOT)/ANEWZ$
```

```
      ESNZMN(1,2)=ESNZTP(1,2)/PHI
      X$=11000.
      M=100000./DELTAX
C**   SURFACE AND MEAN VERTICAL STRAIN RATE AT X=11000     **C
C**   METERS THROUGH X=91000 METERS AT 10000 METER         **C
C**   INTERVALS                                            **C
      DO 6 I=2,M
      ESNZTP(I,I+1)=US(I,I+1)/Q/X$+PHI*(ABL+ZDOT)/Z(1,I+1)
      ESNZMN(I,I+1)=ESNZTP(1,I+1)/PHI
      X$=X$+DELTAX
    6 CONTINUE
C
C*****************************************************************C
C**                                                             **C
C**   BBBBBBBBBBBBBBBBBBBBBBBBBBBBBBBBBBBBBBBBBBBBBBBBBBBBB    **C
C**   BBBBBBBBBBBBBBBBBBBBBBBBBBBBBBBBBBBBBBBBBBBBBBBBBBBBB    **C
C**                                                             **C
C*****************************************************************C
C
C**   LOOP 1: PARTICLE TRAJECTORIES ARE CALCULATED;        **C
C**   STARTING WITH THE ONE THAT ENDS AT X=11000 METERS    **C
C**   THROUGH THE ONE THAT ENDS AT X=91000 METERS AT       **C
C**   1000 METER INTERVALS                                 **C
      DO 1 J=3,M
      WRITE(6,200) J+1
      DEPTH(J,J+1)=0.
      TIME(J,J+1)=0.
      BDOT(J,J+1)=-AB
      CORFAC(J,J+1)=PHI
      K=J+2
C**   LOOP 2: THE TIME A PARTICLE NEEDS TO TRAVEL ALONG    **C
C**   A PARTICULAR TRAJECTORY                              **C
      DO 2 I=K,99
      X(J,I)=X(J,I-1)+DELTAX
      TXT=TIME(J,I-1)+DELTAX/UMEAN(J,I-1)
      L=M+2
      IF(I.LT.L) BDOT(J,I)=-AB
      IF (I.EQ.L) BDOT(J,I)=0.
      IF (I.GT.L) BDOT(J,I)=AC
C**   LOOP 3: THICKNESS, FLUX, SURFACE AND MEAN VELOCITY,  **C
C**   AND SURFACE AND MEAN VERTICAL STRAIN RATE AT SOME    **C
C**   TIME TXT IN THE PAST, AT 10000 METER INTERVALS       **C
C**   ALONG A PARTICLE TRAJECTORY.  ORIGINALLY TXT IS      **C
C**   ESTIMATED ROUGHLY, BUT BECOMES MORE ACCURATE AS      **C
C**   LOOP 3 IS REPEATED                                   **C
      DO 3 LX=1,99
      IF(I.LE.L) Z(J,I)=A*X(J,1)**(1./Q)-ZDOT*(TZERO-TXT)
      IF(I.LE.L) R=RX
      IF(I.GT.L) Z(J,I)=A*101000.**(1./Q)-ZDOT*(TZERO-TXT)
      IF(I.GT.L) R=1.E20
      USZ(J,I)=(((US(J,I-1)*(Z(J,I-1)+Z(J,I)))/(4.*R)+PHI*
     >((BDOT(J,I-1)+BDOT(J,I))/2.-ZDOT))*DELTAX+USZ(J,I-1))/
     >(1.-(1.+Z(J,I-1)/Z(J,I))*DELTAX/(4.*R))
      US(J,I)=USZ(J,I)/Z(J,I)
      UMEAN(J,I)=US(J,I)/PHI
      IF(I.LE.L) ESNZMN(J,I)=(ZDOT-BDOT(J,I)+UMEAN(J,I)*A/Q
     >*X(J,I)**(1./Q-1.))/Z(J,I)
      IF(I.GT.L) ESNZMN(J,I)=(ZDOT-BDOT(J,I))/Z(J,I)
      ESNZTP(J,I)=PHI*ESNZMN(J,I)
      DUMMY=CORFAC(J,I-1)
      EXPONT=(ESNZMN(J,I-1)+ESNZMN(J,I))*DELTAX/
     >(UMEAN(J,I-1)+UMEAN(J,I))
C**   LOOP 8: A NEW PARTICLE DEPTH IS FOUND.  DUMMY IS AN  **C
C**   ESTIMATE FOR CORFAC AT THE NEW POSITION, WHICH       **C
C**   BECOMES MORE ACCURATE AS LOOP 8 IS REPEATED          **C
      DO 8 MX=1,99
      DEPTH(J,I)=DEPTH(J,I-1)*EXP(EXPONT)+(2.*(BDOT(J,I)+
     >BDOT(J,I-1))/((CORFAC(J,I-1)+DUMMY)*(ESNZMN(J,I)+
```

```
     >ESNZMN(J,1-1))))*(EXP(EXPONT)-1.)
       CORFAC(J,I)=PHI*(1.-(DEPTH(J,I)/Z(J,1))**(N+1))
       IF(ABS((CORFAC(J,1)-DUMMY)/CORFAC(J,1)).LT.2.E-2) GO
     >TO 9
       DUMMY=CORFAC(J,1)
     8 CONTINUE
     9 TIME(J,I)=2.*DELTAX/(UMEAN(J,I)*CORFAC(J,I)+
      >UMEAN(J,I-1)*CORFAC(J,I-1))+TIME(J,I-1)
       IF(ABS((TIME(J,1)-TXT)/TIME(J,I)).LT.2.E-2)
      >WRITE(6,201)I,X(J,I),Z(J,I),DEPTH(J,I),CORFAC(J,1),
      >TIME(J,1),US(J,1),ESNZTP(J,1)
       IF(ABS((TIME(J,I)-TXT)/TIME(J,1)).LT.2.E-2) GO TO 4
       TXT=TIME(J,I)
     3 CONTINUE
       WRITE(6,201)I,X(J,I),Z(J,I),DEPTH(J,I),CORFAC(J,1),
      >TIME(J,I),US(J,I),ESNZTP(J,I)
     4 IF (DEPTH(J,I).LE.0.) GO TO 1
     2 CONTINUE
     1 CONTINUE
C
C*****************************************************************C
C**                                                             **C
C**  CCCCCCCCCCCCCCCCCCCCCCCCCCCCCCCCCCCCCCCCCCCCCCCCCCCCCCCC  **C
C**  CCCCCCCCCCCCCCCCCCCCCCCCCCCCCCCCCCCCCCCCCCCCCCCCCCCCCCCC  **C
C**                                                             **C
C*****************************************************************C
C
C**  LOOP 10: METEORITE CONCENTRATION STARTING AT               **C
C**  X=11000 METERS THROUGH X=91000 METERS AT 10000             **C
C**  METER INTERVALS                                            **C
       DO 10 I=1,M
       R=RX
       TOLD=0.
       WRITE(6,208)
       MXM=M+1
       IP=I+1
C**  LOOP 11: THE MAXIMUM AMOUNT OF TIME A METEORITE            **C
C**  HAS TRAVELLED ALONG THE ABLATION SURFACE, STARTING         **C
C**  WITH A METEORITE FOUND AT X=11000 METERS THROUGH           **C
C**  ONE FOUND AT X=91000 METERS AT 10000 METER                 **C
C**  INTERVALS                                                  **C
       DO 11 J=IP,MXM
       US(I,J+1)=US(J,J+1)
       X(I,J+1)=X(J,J+1)
       IF(J.LT.MXM) BDOTN=-AB
       IF(J.EQ.MXM) BDOTN=-(AB/2.)
       TORIG=2.*DELTAX/(US(I,J+1)+US(1,J))+TOLD
       TNEW=TORIG
C**  LOOP 12: PROCEDURE TO MAKE THE CALCULATION FOR             **C
C**  THE MAXIMUM AMOUNT OF TIME A METEORITE HAS                 **C
C**  TRAVELLED ALONG THE ABLATION SURFACE MORE ACCURATE         **C
       DO 12 MN=1,99
       Z(I,J+1)=A*X(I,J+1)**(1./Q)-ZDOT*(TZERO-TNEW)
       USZ(I,J+1)=((US(I,J)*(Z(I,J)+Z(I,J+1)))/(4.*R)+PHI*
      >(BDOTN-ZDOT))*DELTAX+USZ(1,J))/(1.-(1.+Z(I,J)/Z(I,J+1)
      >)*DELTAX/(4.*R))
       US(I,J+1)=USZ(I,J+1)/Z(I,J+1)
       TNEW=2.*DELTAX/(US(I,J+1)+US(I,J))+TOLD
       IF(ABS((TNEW-TORIG)/TNEW).LT.2.E-2) GO TO 13
    12 CONTINUE
       IF(J.LT.MXM) ABL=AB
       IF(J.EQ.MXM) ABL=0.
    13 ESNXSY(I,J+1)=-US(I,J+1)/Q/X(I,J+1)-PHI*
      >(ABL+ZDOT)/Z(I,J+1)
       TOLD=TNEW
    11 CONTINUE
       ABL=AB
       ESNXSY(I,I+1)=-ESNZTP(1,I+1)
```

```
      CONCTN(I,MXM+1)=0.
      KLK=11-1
C**   LOOP 14: METEORITE CONCENTRATION STARTING AT          **C
C**   X=11000 METERS THROUGH X=91000 METERS AT 10000        **C
C**   METER INTERVALS                                       **C
      DO 14 KL=1,KLK
      KZ=12-KL
      CONCTN(I,KZ)=(-(F+F*ABL/AC-(ESNX$Y(I,KZ)+ESNX$Y(I,KZ+1
     >))*CONCTN(I,KZ+1)/4.)*2.*DELTAX/(US(I,KZ)+US(I,KZ+1))+
     >CONCTN(I,KZ+1))/(1.-(ESNX$Y(I,KZ)+ESNX$Y(I,KZ+1))*
     >DELTAX/2./(US(I,KZ)+US(I,KZ+1)))
   14 CONTINUE
      MXMX=MXM+1
      DO 15 KM=1P,MXMX
      WRITE(6,206) KM,X(I,KM),CONCTN(I,KM),US(I,KM),
     >ESNX$Y(I,KM)
      IF (KM.EQ.12) WRITE(6,207) TNEW
   15 CONTINUE
   10 CONTINUE
C
C*****************************************************************C
C**                                                             **C
C**   DDDDDDDDDDDDDDDDDDDDDDDDDDDDDDDDDDDDDDDDDDDDDDDDDDDDD   **C
C**   DDDDDDDDDDDDDDDDDDDDDDDDDDDDDDDDDDDDDDDDDDDDDDDDDDDDD   **C
C**                                                             **C
C*****************************************************************C
C
```

```
  200 FORMAT(////' START OF TRAJECTORY AT I=',I2/'0',
     >'POSITION #',3X,'DISTANCE SNOUT',3X,
     >'THICKNESS GLACIER',3X,'DEPTH PARTICLE',
     >3X,'PSI',3X,'TIME ELAPSED',3X,'SURFACE VELOCITY',3X,
     >'SURFACE VERT. STRAIN RATE')
  201 FORMAT (I6,F17.0,2F19.3,F9.2,2F14.2,G25.3)
  206 FORMAT (I6,F17.0,G18.3,F15.2,G29.3)
  207 FORMAT(85X,F32.3)
  208 FORMAT (////' METEORITE CONCENTRATIONS'/'0',
     >'POSITION #',3X,'DISTANCE SNOUT',3X,'CONCENTRATION',
     >3X,'SURFACE VELOCITY',3X,
     >'SUM HORIZ. SURF. STRAIN RATES',3X,
     >'MAX. TIME ALONG ABLATION SURFACE')
      STOP
      END
```

APPENDIX D

Sample output and graphs

EXPLANATION OF COMPUTER OUTPUT:

In the computer program listed, I is a position indicator. I = 4 represents a distance from the snout of 21,000 m, I = 5 is equalivent to a distance of 31,000 m, etc.

The part of the output that lists the meteorite concentrations at various distances from the snout is repetitious, except for the last column of that output. This column gives the maximum possible time (in years) for subaerial weathering for meteorites at the underlined distances from the snout.

START OF TRAJECTORY AT I= 4

POSITION #	DISTANCE SNOUT	THICKNESS GLACIER	DEPTH PARTICLE	PSI	TIME ELAPSED	SURFACE VELOCITY	SURFACE VERT. STRAIN RATE
5	31000.	1401.759	275.973	1.44	-4732.51	-2.32	0.606E-05
6	41000.	1728.781	525.452	1.36	-9067.05	-2.63	0.402E-05
7	51000.	2036.243	763.692	1.29	-13148.74	-2.93	0.114E-05
8	61000.	2328.893	976.777	1.24	-17007.61	-3.24	-0.114E-05
9	71000.	2609.730	1202.602	1.18	-20667.02	-3.55	-0.305E-05
10	81000.	2880.818	1425.247	1.13	-24155.14	-3.89	-0.474E-05
11	91000.	3143.641	1645.393	1.09	-27482.51	-4.24	-0.629E-05
12	101000.	3399.328	1818.824	1.07	-30674.51	-4.47	-0.33ZE-04
13	111000.	3399.328	1861.855	1.05	-33870.44	-4.38	-0.172E-04
14	121000.	3399.328	1807.313	1.08	-37155.09	-4.21	-0.172E-04
15	131000.	3399.328	1751.361	1.10	-40495.36	-4.04	-0.172E-04
16	141000.	3399.328	1693.644	1.13	-43900.30	-3.87	-0.172E-04
17	151000.	3399.328	1633.765	1.15	-47379.60	-3.69	-0.172E-04
18	161000.	3399.328	1571.271	1.18	-50943.82	-3.52	-0.172E-04
19	171000.	3399.328	1505.632	1.21	-54604.63	-3.35	-0.172E-04
20	181000.	3399.328	1436.221	1.23	-58375.12	-3.18	-0.172E-04
21	191000.	3399.328	1362.282	1.26	-62270.22	-3.01	-0.172E-04
22	201000.	3399.328	1282.888	1.29	-66307.19	-2.83	-0.172E-04
23	211000.	3399.328	1196.878	1.31	-70506.38	-2.66	-0.172E-04
24	221000.	3399.328	1102.776	1.34	-74892.13	-2.49	-0.172E-04
25	231000.	3399.328	998.662	1.37	-79494.06	-2.32	-0.172E-04
26	241000.	3399.328	881.982	1.40	-84349.13	-2.15	-0.172E-04
27	251000.	3399.328	747.115	1.43	-89503.81	-1.97	-0.172E-04
28	261000.	3399.328	591.145	1.45	-95019.94	-1.80	-0.172E-04
29	271000.	3399.328	406.955	1.48	-100983.70	-1.63	-0.172E-04
30	281000.	3399.328	183.787	1.50	-107520.50	-1.46	-0.172E-04
31	291000.	3399.328	-95.499	1.50	-114825.80	-1.29	-0.172E-04

START OF TRAJECTORY AT I= 5

POSITION #	DISTANCE SNOUT	THICKNESS GLACIER	DEPTH PARTICLE	PSI	TIME ELAPSED	SURFACE VELOCITY	SURFACE VERT. STRAIN RATE
6	41000.	1728.781	239.649	1.47	-4084.81	-2.63	0.402E-05
7	51000.	2036.243	460.223	1.42	-7820.07	-2.93	0.114E-05
8	61000.	2328.893	652.100	1.38	-11291.88	-3.24	-0.114E-05
9	71000.	2609.730	851.405	1.34	-14540.09	-3.55	-0.305E-05
10	81000.	2880.818	1044.328	1.30	-17593.25	-3.89	-0.474E-05
11	91000.	3143.641	1232.012	1.27	-20466.33	-4.24	-0.629E-05
12	101000.	3399.328	1372.459	1.26	-23196.15	-4.47	-0.33ZE-04
13	111000.	3399.328	1398.696	1.25	-25905.55	-4.38	-0.172E-04
14	121000.	3399.328	1344.375	1.27	-28685.85	-4.21	-0.172E-04
15	131000.	3399.328	1287.203	1.28	-31538.02	-4.04	-0.172E-04
16	141000.	3399.328	1226.759	1.30	-34469.26	-3.87	-0.172E-04
17	151000.	3399.328	1162.550	1.32	-37487.73	-3.69	-0.172E-04
18	161000.	3399.328	1093.982	1.34	-40602.79	-3.52	-0.172E-04
19	171000.	3399.328	1020.342	1.36	-43825.21	-3.35	-0.172E-04
20	181000.	3399.328	940.756	1.39	-47167.61	-3.18	-0.172E-04
21	191000.	3399.328	854.147	1.41	-50644.89	-3.01	-0.172E-04
22	201000.	3399.328	759.164	1.43	-54274.99	-2.83	-0.172E-04
23	211000.	3399.328	654.089	1.44	-58079.76	-2.66	-0.172E-04
24	221000.	3399.328	536.699	1.46	-62086.44	-2.49	-0.172E-04
25	231000.	3399.328	404.055	1.48	-66329.75	-2.32	-0.172E-04
26	241000.	3399.328	252.192	1.49	-70855.25	-2.15	-0.172E-04
27	251000.	3399.328	75.609	1.50	-75725.00	-1.97	-0.172E-04
28	261000.	3399.328	-133.583	1.50	-81027.50	-1.80	-0.172E-04

START OF TRAJECTORY AT I= 6

POSITION #	DISTANCE SNOUT	THICKNESS GLACIER	DEPTH PARTICLE	PSI	TIME ELAPSED	SURFACE VELOCITY	SURFACE VERT. STRAIN RATE
7	51000.	2036.243	215.044	1.48	-3622.02	-2.93	0.114E-05
8	61000.	2328.893	387.578	1.46	-6932.35	-3.24	-0.114E-05
9	71000.	2609.730	574.249	1.43	-9996.33	-3.55	-0.305E-05
10	81000.	2880.818	752.445	1.40	-12852.52	-3.89	-0.474E-05
11	91000.	3143.641	922.365	1.37	-15521.78	-4.24	-0.629E-05
12	101000.	3399.328	1042.296	1.36	-18046.77	-4.47	-0.33ZE-04
13	111000.	3399.328	1053.316	1.36	-20543.24	-4.38	-0.172E-04

14	121000.	3399.328	993.920	1.37	-23102.97	-4.21	-0.172E-04
15	131000.	3399.328	930.693	1.39	-25738.98	-4.04	-0.172E-04
16	141000.	3399.328	863.095	1.40	-28458.68	-3.87	-0.172E-04
17	151000.	3399.328	790.481	1.42	-31270.62	-3.69	-0.172E-04
18	161000.	3399.328	712.073	1.43	-34184.77	-3.52	-0.172E-04
19	171000.	3399.328	626.926	1.45	-37212.91	-3.35	-0.172E-04
20	181000.	3399.328	533.872	1.46	-40369.14	-3.18	-0.172E-04
21	191000.	3399.328	431.455	1.48	-43670.54	-3.01	-0.172E-04
22	201000.	3399.328	317.833	1.49	-47138.27	-2.83	-0.172E-04
23	211000.	3399.328	190.635	1.50	-50799.03	-2.66	-0.172E-04
24	221000.	3399.328	46.753	1.50	-54687.46	-2.49	-0.172E-04
25	231000.	3399.328	-117.982	1.50	-58849.91	-2.32	-0.172E-04

START OF TRAJECTORY AT I= 7

POSITION #	DISTANCE SNOUT	THICKNESS GLACIER	DEPTH PARTICLE	PSI	TIME ELAPSED	SURFACE VELOCITY	SURFACE VERT. STRAIN RATE
8	61000.	2328.893	167.486	1.49	-3253.50	-3.24	-0.114E-05
9	71000.	2609.730	346.734	1.47	-6234.27	-3.55	-0.305E-05
10	81000.	2880.818	515.437	1.45	-8991.99	-3.89	-0.474E-05
11	91000.	3143.641	676.145	1.43	-11555.39	-4.24	-0.629E-05
12	101000.	3399.328	781.434	1.42	-13972.72	-4.47	-0.334E-04
13	111000.	3399.328	779.347	1.42	-16357.72	-4.38	-0.172E-04
14	121000.	3399.328	713.455	1.43	-18803.22	-4.21	-0.172E-04
15	131000.	3399.328	642.855	1.45	-21328.46	-4.04	-0.172E-04
16	141000.	3399.328	566.881	1.46	-23941.54	-3.87	-0.172E-04
17	151000.	3399.328	484.726	1.47	-26651.96	-3.69	-0.172E-04
18	161000.	3399.328	395.414	1.48	-29470.99	-3.52	-0.172E-04
19	171000.	3399.328	297.751	1.49	-32412.22	-3.35	-0.172E-04
20	181000.	3399.328	190.250	1.50	-35492.28	-3.18	-0.172E-04
21	191000.	3399.328	71.041	1.50	-38731.88	-3.01	-0.172E-04
22	201000.	3399.328	-62.266	1.50	-42157.46	-2.83	-0.172E-04

START OF TRAJECTORY AT I= 8

POSITION #	DISTANCE SNOUT	THICKNESS GLACIER	DEPTH PARTICLE	PSI	TIME ELAPSED	SURFACE VELOCITY	SURFACE VERT. STRAIN RATE
9	71000.	2609.730	177.288	1.49	-2953.02	-3.55	-0.305E-05
10	81000.	2880.818	342.044	1.48	-5667.34	-3.89	-0.474E-05
11	91000.	3143.641	497.589	1.46	-8179.40	-4.24	-0.629E-05
12	101000.	3399.328	592.988	1.45	-10542.46	-4.47	-0.332E-04
13	111000.	3399.328	580.968	1.46	-12871.22	-4.38	-0.172E-04
14	121000.	3399.328	509.321	1.47	-15260.25	-4.21	-0.172E-04
15	131000.	3399.328	432.257	1.46	-17732.39	-4.04	-0.172E-04
16	141000.	3399.328	348.994	1.48	-20296.58	-3.67	-0.172E-04
17	151000.	3399.328	258.587	1.49	-22963.43	-3.69	-0.172E-04
18	161000.	3399.328	159.883	1.50	-25745.75	-3.52	-0.172E-04
19	171000.	3399.328	51.463	1.50	-28659.21	-3.35	-0.172E-04
20	181000.	3399.328	-68.448	1.50	-31723.41	-3.18	-0.172E-04

START OF TRAJECTORY AT I= 9

POSITION #	DISTANCE SNOUT	THICKNESS GLACIER	DEPTH PARTICLE	PSI	TIME ELAPSED	SURFACE VELOCITY	SURFACE VERT. STRAIN RATE
10	81000.	2880.818	162.138	1.50	-2692.81	-3.89	-0.474E-05
11	91000.	3143.641	313.570	1.49	-5171.72	-4.24	-0.629E-05
12	101000.	3399.328	399.329	1.48	-7496.79	-4.47	-0.332E-04
13	111000.	3399.328	376.753	1.48	-9785.95	-4.38	-0.172E-04
14	121000.	3399.328	298.396	1.49	-12136.71	-4.21	-0.172E-04
15	131000.	3399.328	213.813	1.49	-14575.27	-4.04	-0.172E-04
16	141000.	3399.328	122.088	1.50	-17111.79	-3.87	-0.172E-04
17	151000.	3399.328	22.102	1.50	-19758.53	-3.69	-0.172E-04
18	161000.	3399.328	-87.513	1.50	-22530.55	-3.52	-0.172E-04

START OF TRAJECTORY AT I=10

POSITION #	DISTANCE SNOUT	THICKNESS GLACIER	DEPTH PARTICLE	PSI	TIME ELAPSED	SURFACE VELOCITY	SURFACE VERT. STRAIN RATE
11	91000.	3143.641	148.743	1.50	-2465.16	-4.24	-0.629E-05
12	101000.	3399.328	226.306	1.49	-4770.26	-4.47	-0.332E-04
13	111000.	3399.328	194.027	1.50	-7038.29	-4.38	-0.172E-04
14	121000.	3399.328	109.053	1.50	-9370.50	-4.21	-0.172E-04
15	131000.	3399.328	17.054	1.50	-11796.05	-4.04	-0.172E-04
16	141000.	3399.328	-83.028	1.50	-14326.61	-3.87	-0.172E-04

START OF TRAJECTORY AT I=11

POSITION #	DISTANCE SNOUT	THICKNESS GLACIER	DEPTH PARTICLE	PSI	TIME ELAPSED	SURFACE VELOCITY	SURFACE VERT. STRAIN RATE
12	101000.	3399.328	70.505	1.50	-2297.85	-4.47	-0.332E-04
13	111000.	3399.328	29.282	1.50	-4557.72	-4.38	-0.172E-04
14	121000.	3399.328	-62.129	1.50	-6885.34	-4.21	-0.172E-04

METEORITE CONCENTRATIONS

POSITION #	DISTANCE SNOUT	CONCENTRATION	SURFACE VELOCITY	SUM HORIZ. SURF. STRAIN RATES	MAX. TIME ALONG ABLATION SURFACE
2	1000.	0.189E-04	-0.85	-0.209E-03	
3	11000.	0.567E-05	-1.61	-0.300E-04	
4	21000.	0.421E-05	-2.00	-0.147E-04	
5	31000.	0.331E-05	-2.32	-0.806E-05	
6	41000.	0.262E-05	-2.63	-0.402E-05	
7	51000.	0.205E-05	-2.93	-0.114E-05	
8	61000.	0.156E-05	-3.24	0.114E-05	
9	71000.	0.111E-05	-3.55	0.305E-05	
10	81000.	0.715E-06	-3.89	0.474E-05	
11	91000.	0.347E-06	-4.24	0.629E-05	
12	101000.	0.000	-4.47	0.671E-05	
					-39617.560

METEORITE CONCENTRATIONS

POSITION #	DISTANCE SNOUT	CONCENTRATION	SURFACE VELOCITY	SUM HORIZ. SURF. STRAIN RATES	MAX. TIME ALONG ABLATION SURFACE
3	11000.	0.567E-05	-1.61	-0.300E-04	
4	21000.	0.421E-05	-2.00	-0.147E-04	
5	31000.	0.331E-05	-2.32	-0.806E-05	
6	41000.	0.262E-05	-2.63	-0.402E-05	
7	51000.	0.205E-05	-2.93	-0.114E-05	
8	61000.	0.156E-05	-3.24	0.114E-05	
9	71000.	0.111E-05	-3.55	0.305E-05	
10	81000.	0.715E-06	-3.89	0.474E-05	
11	91000.	0.347E-06	-4.24	0.629E-05	
12	101000.	0.000	-4.47	0.671E-05	
					-31466.400

METEORITE CONCENTRATIONS

POSITION #	DISTANCE SNOUT	CONCENTRATION	SURFACE VELOCITY	SUM HORIZ. SURF. STRAIN RATES	MAX. TIME ALONG ABLATION SURFACE
4	21000.	0.421E-05	-2.00	-0.147E-04	
5	31000.	0.331E-05	-2.32	-0.806E-05	
6	41000.	0.262E-05	-2.63	-0.402E-05	
7	51000.	0.205E-05	-2.93	-0.114E-05	
8	61000.	0.156E-05	-3.24	0.114E-05	
9	71000.	0.111E-05	-3.55	0.305E-05	
10	81000.	0.715E-06	-3.89	0.474E-05	
11	91000.	0.347E-06	-4.24	0.629E-05	
12	101000.	0.000	-4.47	0.671E-05	
					-25916.250

METEORITE CONCENTRATIONS

POSITION #	DISTANCE SNOUT	CONCENTRATION	SURFACE VELOCITY	SUM HORIZ. SURF. STRAIN RATES	MAX. TIME ALONG ABLATION SURFACE
5	31000.	0.331E-05	-2.32	-0.606E-05	
6	41000.	0.262E-05	-2.63	-0.402E-05	
7	51000.	0.205E-05	-2.93	-0.114E-05	
8	61000.	0.156E-05	-3.24	0.114E-05	
9	71000.	0.111E-05	-3.55	0.305E-05	
10	81000.	0.715E-06	-3.89	0.474E-05	
11	91000.	0.347E-06	-4.24	0.629E-05	
12	101000.	0.000	-4.47	0.671E-05	
					-21262.360

METEORITE CONCENTRATIONS

POSITION #	DISTANCE SNOUT	CONCENTRATION	SURFACE VELOCITY	SUM HORIZ. SURF. STRAIN RATES	MAX. TIME ALONG ABLATION SURFACE
6	41000.	0.262E-05	-2.63	-0.402E-05	
7	51000.	0.205E-05	-2.93	-0.114E-05	
8	61000.	0.156E-05	-3.24	0.114E-05	
9	71000.	0.111E-05	-3.55	0.305E-05	
10	81000.	0.715E-06	-3.89	0.474E-05	
11	91000.	0.347E-06	-4.24	0.629E-05	
12	101000.	0.000	-4.47	0.671E-05	
					-17239.230

METEORITE CONCENTRATIONS

POSITION #	DISTANCE SNOUT	CONCENTRATION	SURFACE VELOCITY	SUM HORIZ. SURF. STRAIN RATES	MAX. TIME ALONG ABLATION SURFACE
7	51000.	0.205E-05	-2.93	-0.114E-05	
8	61000.	0.156E-05	-3.24	0.114E-05	
9	71000.	0.111E-05	-3.55	0.305E-05	
10	81000.	0.715E-06	-3.89	0.474E-05	
11	91000.	0.347E-06	-4.24	0.629E-05	
12	101000.	0.000	-4.47	0.671E-05	
					-13636.516

METEORITE CONCENTRATIONS

POSITION #	DISTANCE SNOUT	CONCENTRATION	SURFACE VELOCITY	SUM HORIZ. SURF. STRAIN RATES	MAX. TIME ALONG ABLATION SURFACE
8	61000.	0.156E-05	-3.24	0.114E-05	
9	71000.	0.111E-05	-3.55	0.305E-05	
10	81000.	0.715E-06	-3.89	0.474E-05	
11	91000.	0.347E-06	-4.24	0.629E-05	
12	101000.	0.000	-4.47	0.671E-05	
					-10393.650

METEORITE CONCENTRATIONS

POSITION #	DISTANCE SNOUT	CONCENTRATION	SURFACE VELOCITY	SUM HORIZ. SURF. STRAIN RATES	MAX. TIME ALONG ABLATION SURFACE
9	71000.	0.111E-05	-3.55	0.305E-05	
10	81000.	0.715E-06	-3.89	0.474E-05	
11	91000.	0.347E-06	-4.24	0.629E-05	
12	101000.	0.000	-4.47	0.671E-05	
					-7447.977

METEORITE CONCENTRATIONS

POSITION #	DISTANCE SNOUT	CONCENTRATION	SURFACE VELOCITY	SUM HORIZ. SURF. STRAIN RATES	MAX. TIME ALONG ABLATION SURFACE
10	81000.	0.715E-06	-3.89	0.474E-05	
11	91000.	0.347E-06	-4.24	0.629E-05	
12	101000.	0.000	-4.47	0.671E-05	
					-4759.621

METEORITE CONCENTRATIONS

POSITION #	DISTANCE SNOUT	CONCENTRATION	SURFACE VELOCITY	SUM HORIZ. SURF. STRAIN RATES	MAX. TIME ALONG ABLATION SURFACE
11	91000.	0.347E-06	-4.24	0.629E-05	
12	101000.	0.000	-4.47	0.671E-05	
					-2297.339

GRAPHS

The following are graphs of values listed
in the sample output

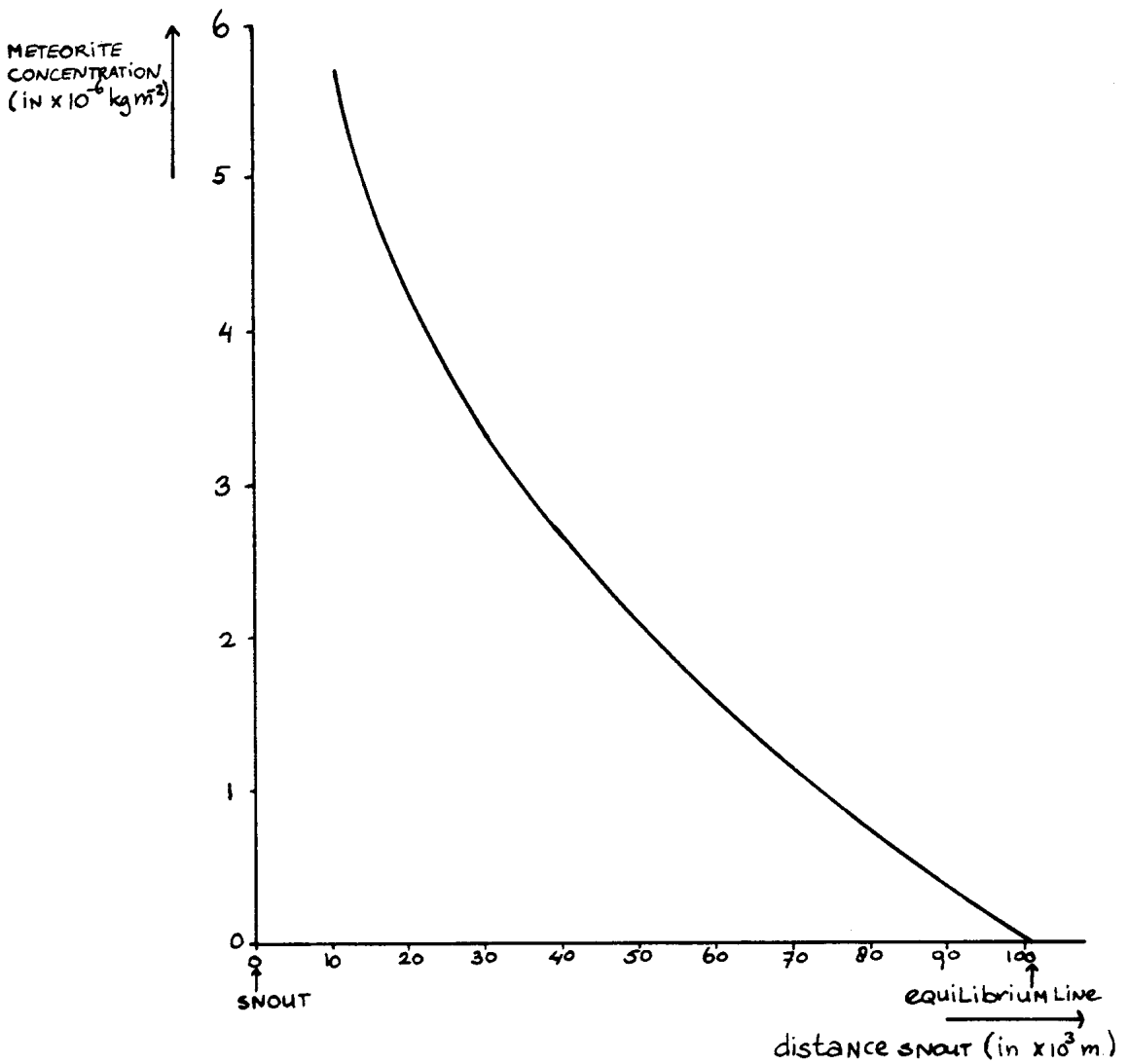

Figure 9. Meteorite concentration versus distance from the snout.

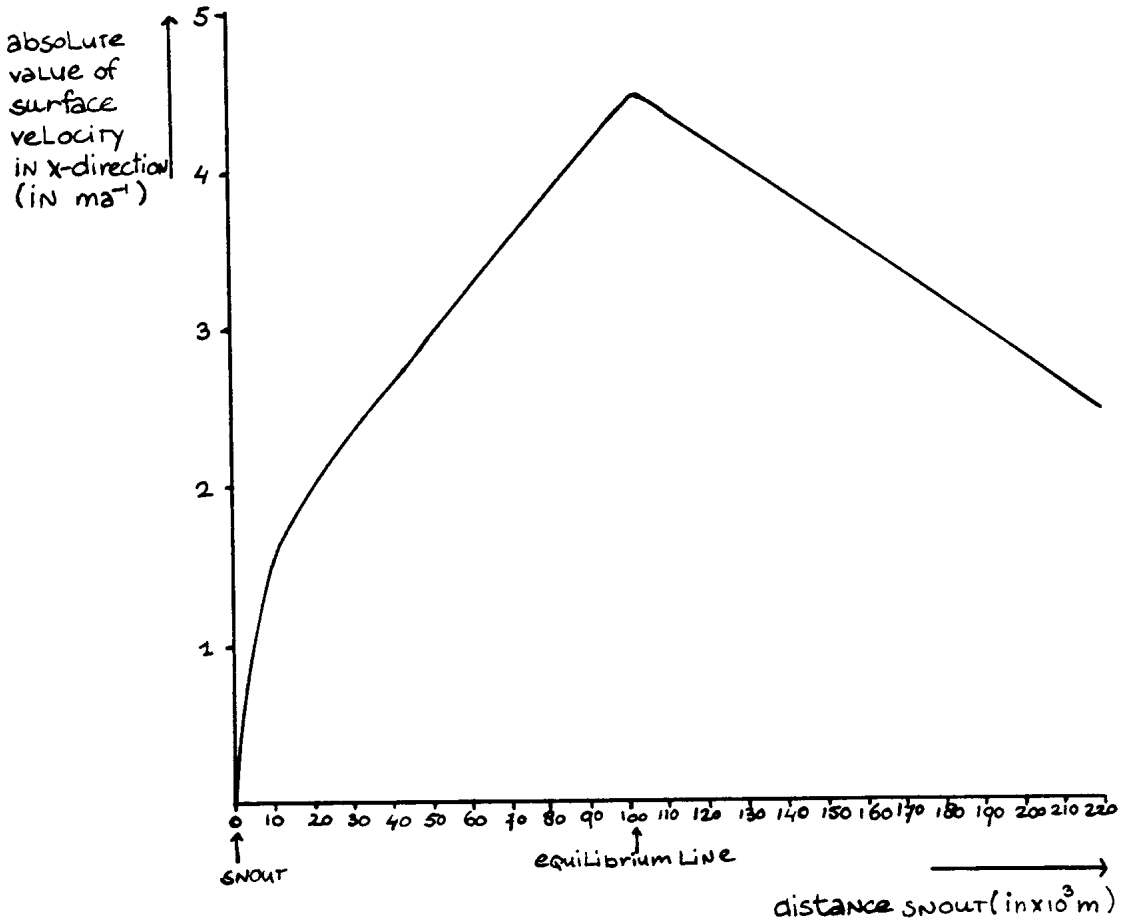

Figure 10. Absolute value of the surface velocity versus distance from the snout.

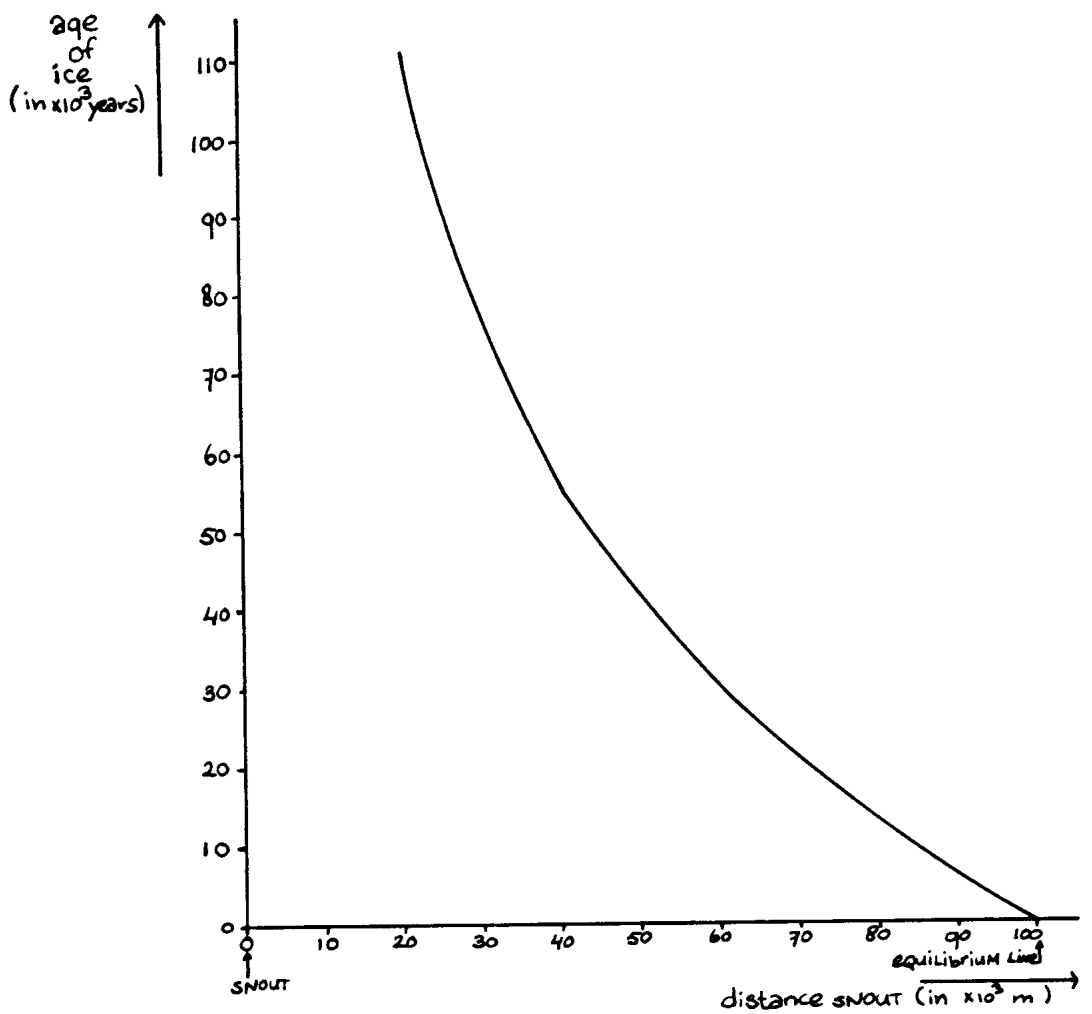

Figure 11. Age of ice at the surface of the ablation zone versus distance from the snout.

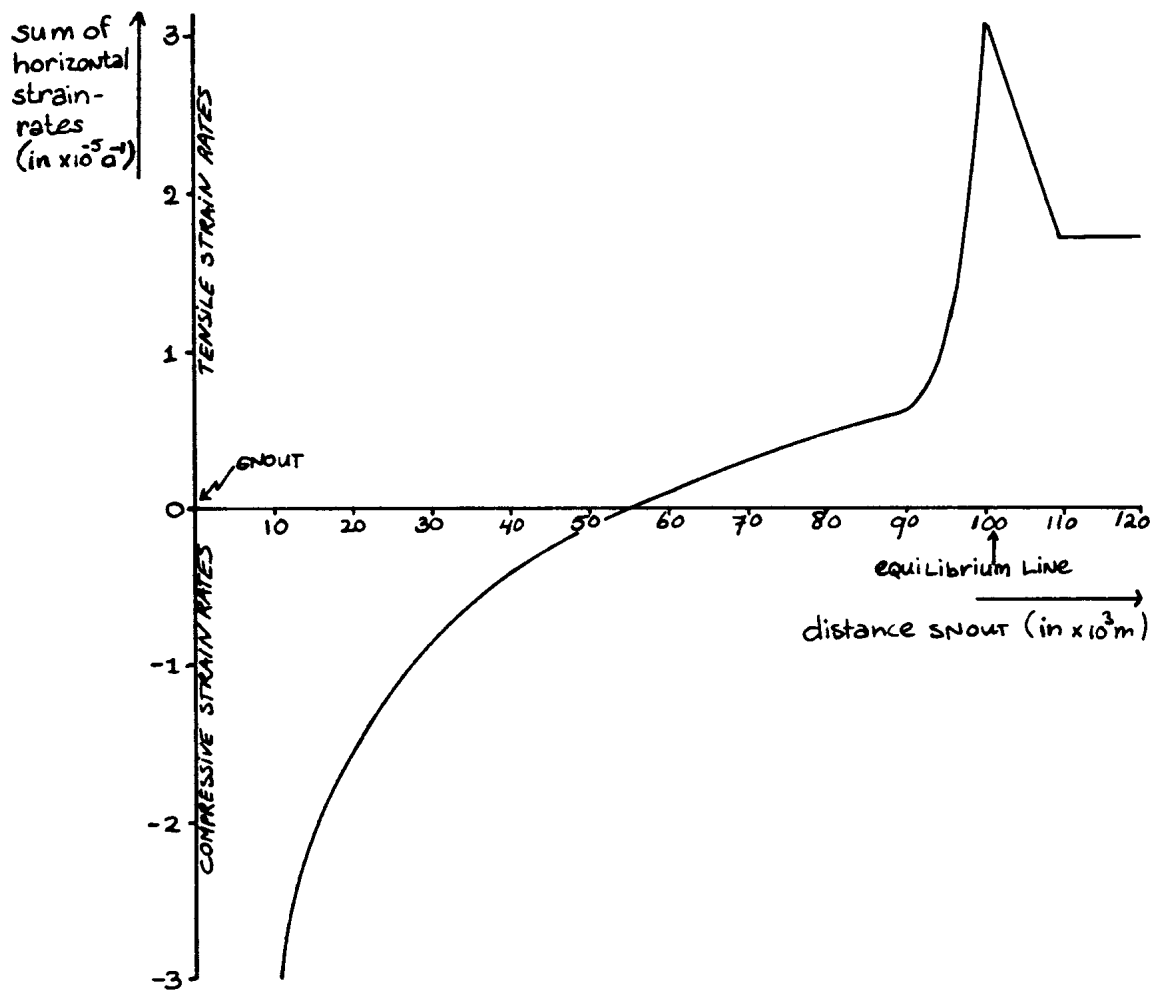

Figure 12. Sum of the horizontal strain rates versus distance from the snout. The peak near the equilibrium line position results from the sudden change in mass balance ($\dot{b}$), used in the computer program. This peak is not present at a real glacier and does not affect the calculated results significantly.

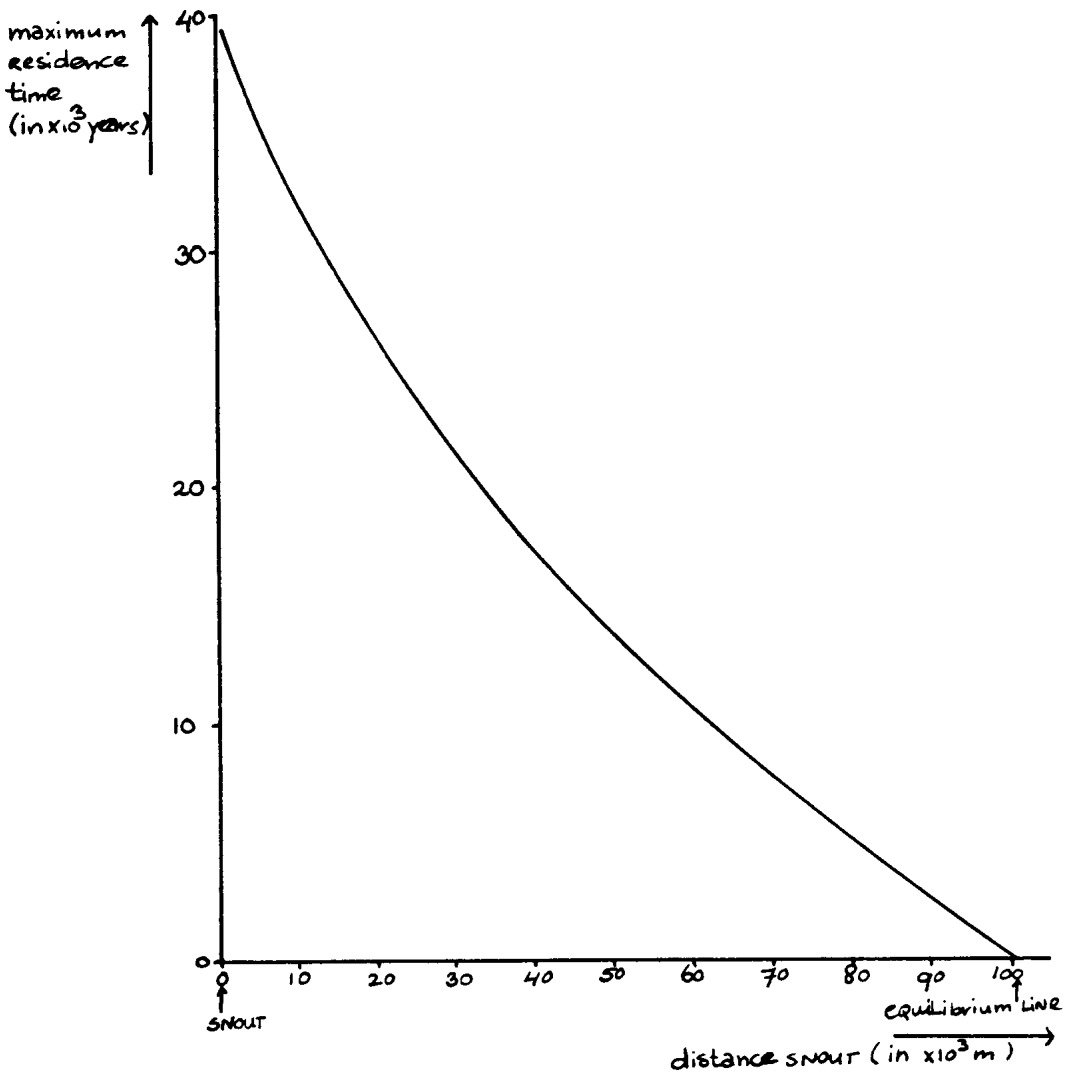

Figure 13. The maximum residence time at the surface of the ablation zone of meteorites versus distance from the snout. Steady state conditions are assumed.

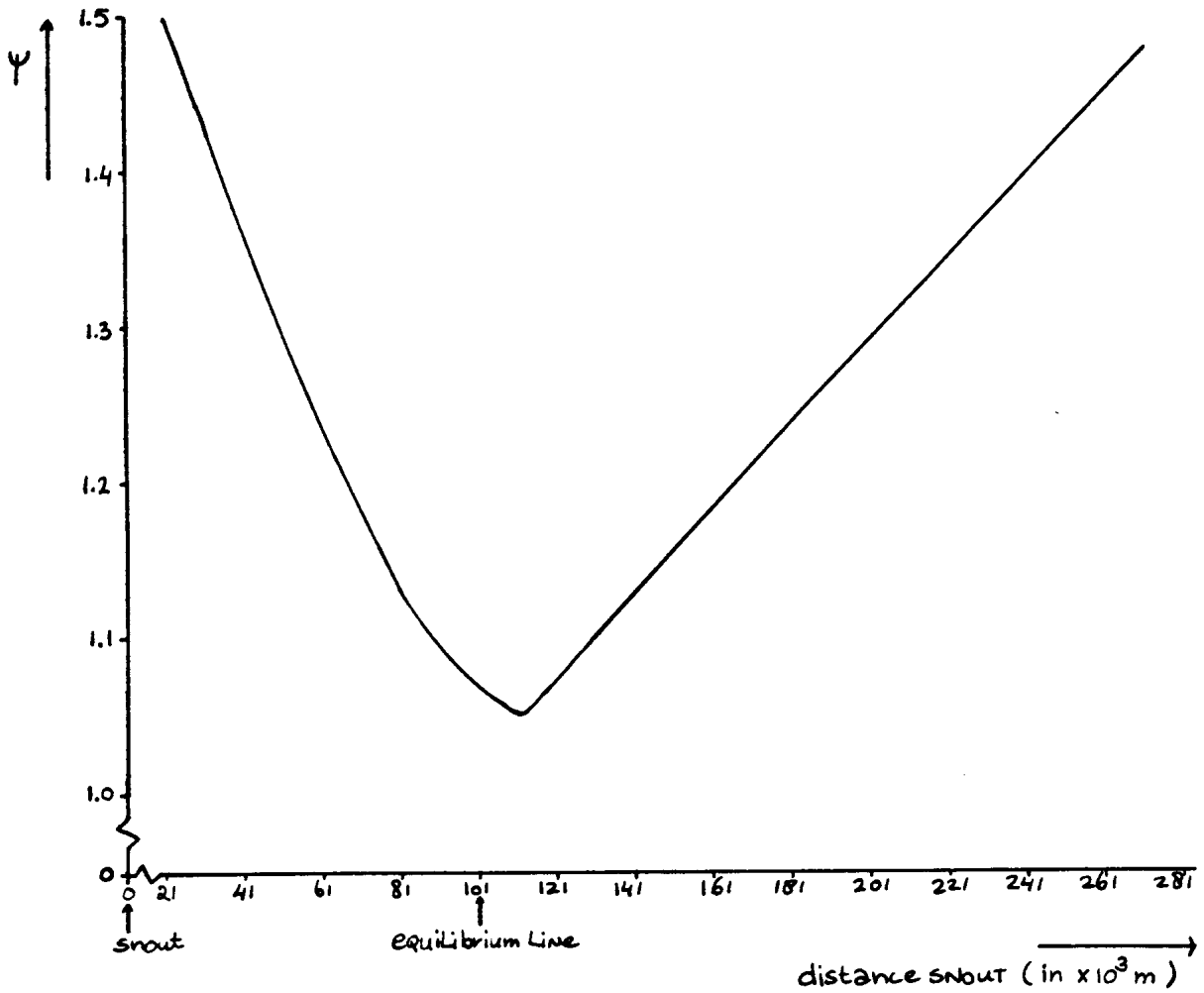

Figure 14. Values of factor ψ at various distances from the snout along the trajectory that emerges at 21,000 m from the snout.